Neural mechanism of rebooting the unconsciousness caused by midazolam

LeYuan Gu[1,2#], WeiHui Shao[2#], Lu Liu[1#], Qing Xu[1#], YuLing Wang[2#], JiaXuan Gu[2#], Yue Yang[2], ZhuoYue Zhang[1], YaXuan Wu[2], Yue Shen[3], Qian Yu[2], XiTing Lian[1], Haixiang Ma[5], YuanLi Zhang[2], HongHai Zhang[1,2,3,4]*

[1]Department of Anesthesiology, Zhejiang University School of Medicine, Hangzhou, 310006, China

[2]Department of Anesthesiology, the Fourth Clinical School of Medicine, Zhejiang Chinese Medical University, Hangzhou, 310006, China

[3]Department of Anesthesiology, Affiliated Hangzhou First People's Hospital, Westlake University School of Medicine, Hangzhou, 310006, China

[4]Westlake Laboratory of Life Sciences and Biomedicine, Hangzhou, 310006, China

[5]Medical College of Jining Medical University, Ningji, 272067, Shandong, China

[#]These authors contributed equally to this work

Corresponding authors: HongHai Zhang

Email address: zhanghonghai_0902@163.com & zhh0902@zju.edu.cn

ORCID: http://orcid.org/0000-0003-3530-2060

Abstract

The advent of midazolam has significant implications for modern clinical practice. The hypnotic and sedative effects of midazolam give it a wide range of clinical utility. However, the specific mechanisms underlying the modulation of altered consciousness by midazolam remain unknown. Herein, using pharmacology, optogenetics, chemogenetics, fiber photometry, and gene knockdown, we revealed the role of locus coeruleus (LC)-ventrolateral preoptic nucleus (VLPO) noradrenergic neural circuit in regulating midazolam-induced altered consciousness. This effect was mediated by α1 adrenergic receptors. Moreover, gamma-aminobutyric acid receptor type A (GABAA-R) is a mechanistically important binding site in the LC for midazolam. Our findings will provide novel insights into the neural circuit mechanisms underlying the recovery of consciousness after midazolam administration and will help guide the timing of clinical dosing and propose effective intervention targets for timely recovery from midazolam-induced loss of consciousness.

Keywords: Midazolam; locus coeruleus (LC); norepinephrine (NE); ventrolateral preoptic nucleus (VLPO); gamma-aminobutyric acid receptor type A (GABAA-R); consciousness

Introduction

Midazolam has been widely used in clinical practice for almost fifty years. It is a short-acting benzodiazepine that has a rapid onset and short duration of action and causes relatively mild hemodynamic effects[1, 2]. It leads to anterograde amnesia and prevents intraoperative awareness and the development of malignant memories in patients. The above characteristics of midazolam make it an indispensable drug for the treatment of psychiatric patients in the United States, China, Europe, and other countries around the world[3].

Psychiatric disorders are a common cause of severe and long-term disability and

socioeconomic burden worldwide. Insomnia is one of the most prevalent health concerns in the population and clinical practice[4]. The World Health Organization (WHO) reported that about 30% of the adult population worldwide suffer from insomnia, especially alongside other mental and physical health conditions[5]. Intractable insomnia occurs comorbidly with other serious complications such as cognitive and immune decline, emotional disorders, and even suicide[6, 7]. Oral benzodiazepines, represented by midazolam, are the cornerstone of their therapy regimen[8]. In addition, agitation is a frequent clinical problem seen in a variety of psychiatric disorders that adds significant morbidity to the hospital course[9]. The extensively used medication for patients with acute agitation in the emergency department and intensive care unit is midazolam[10, 11]. In conclusion, midazolam has become one of the most commonly used psychotropic drugs in clinical practice to induce a sedative response with faded consciousness.

However, a pressing challenge to the application of midazolam in the clinic is the issue of its safety. Depending on the dose, it produces effects ranging from anxiolysis to loss of consciousness, leading it to be versatile to have anxiolytic, sedative and hypnotic effects[12, 13]. Excessive or long-term use of midazolam often causes increased accumulation and depth of sedation, potentially leading to delayed recovery, which in turn prolongs hospitalization and causes various complications[14]. Therefore, it is imperative to explore the mechanisms of midazolam-induced altered consciousness and find promising targets to prevent its complications.

Midazolam has depressant effects on the central nervous system (CNS). It is believed to act on the brainstem reticular formation and limbic system through gamma-aminobutyric acid

receptor type A (GABAA-R) to reduce the excitability in the brain, thereby inducing sedation. GABAA-R is the initiating molecular target of midazolam action. However, the specific mechanism of the regulatory systems downstream of the GABAergic system in midazolam-induced altered consciousness remains to be elucidated. Midazolam can induce a similar pattern of electroencephalographic (EEG) to that seen during normal nonrapid eye movement (NREM) sleep, and neither has a sustained long-range specific activation pattern compared to wakefulness[15]. Therefore, we postulate that a midazolam-induced loss of consciousness, at least in part, via activation of an endogenous sleep-promoting pathway.

The LC is the primary site for norepinephrine (NE) synthesis and release in the brain and has a wide range of projections to other brain regions[16]. The LC^{NE} neurons, which has been linked to multiple functions, including sleep and arousal, stress-related behaviors, attention, and pain conduction, are reportedly instrumental in sleep–arousal regulation[17, 18]. Optogenetic activation of LC^{NE} neurons causes an immediate transition from sleep to wakefulness[19]. The ventrolateral preoptic nucleus (VLPO) of the preoptic hypothalamus is recognized as a key "sleep center" in which sleep-activated neurons are responsible for initiating and promoting sleep and are under the control of the LC^{NE} neurons[20-22]. Recently, it has been reported that optogenetic activation of the LC-VLPO NEergic neural circuit promotes arousal from sleep and acts through different adrenergic receptors, indicating the significance of this neural circuit in controlling wakefulness[23]. However, natural sleep is a physiological state, whereas drug-induced loss of consciousness is a pathological state, and the two are quite different from a pathophysiological perspective despite some correlation. Furthermore, dexmedetomidine-induced sedation involves the endogenous sleep-promoting pathway of

LC-VLPO[24]. Therefore, these studies offer hints for additional investigation into the role of LC-VLPO NEergic neural circuit in midazolam-induced changes in consciousness. This will enable a more targeted clarification of the neural mechanisms underlying the sedative-hypnotic effects of midazolam, which will have significant clinical implications.

In the present study, it was unveiled that midazolam initially functioned by acting on GABAA-R in the LC. More importantly, we found that the LC-VLPO NEergic neural circuit was instrumental in promoting recovery from midazolam and that this effect was primarily mediated by α1 adrenergic receptors (α1-R). We took a cascading approach from peripheral to central to validate our hypothesis. First, we used pharmacology to investigate the link between the NE system and awakening from midazolam administration. On this basis, we then took more precise and specific approaches, such as optogenetics and chemogenetics to further substantiate our finding and successfully prove the involvement of the NEergic LC-VLPO neural circuit in facilitating the restoration of consciousness after midazolam administration. These results will significantly advance the understanding of the neural circuit mechanisms of midazolam-induced altered consciousness and provide a potential target for intervention in the delayed recovery caused by midazolam.

Results

The noradrenergic system is involved in recovery from midazolam administration.

Before starting the following experiments, we first determined the optimal intraperitoneal (IP) dose of midazolam-induced sedation (loss of consciousness). We chose the lowest effective dose that could induce LORR successfully in all of the mice, i.e., 60 mg/kg, as the dose for the subsequent experiments (Figure 1A-B).

To investigate the role of the central noradrenergic system, we individually analyzed the tyrosine hydroxylase (TH) content and activity in the prosencephalon and brainstem of mice (Figure 1C). Since NE in the brain is mainly derived from the brainstem, there were some differences in TH content and activity between the prosencephalon and the brainstem under normal conditions ($P<0.05$, $P<0.001$, Figure 1D). However, we also found that compared with the control group, the TH activity in the brainstem was significantly reduced after midazolam administration ($P<0.0001$, Figure 1D).

Next, we adopted a pharmacological method of peripheral intervention on NE. We found that IP injection of atomoxetine (20 mg/kg), a central selective NE reuptake inhibitor, increased the number of c-Fos (+)/TH (+) cells in the LC ($P < 0.01$, Figure 1J, L) and shortened the recovery time from midazolam administration ($P < 0.05$, Figure 1F). Conversely, IP injection of N-(2-chloroethyl)-N-ethyl-2-bromoben-zylamine hydrochloride (DSP-4) (50 mg/kg), a highly selective NEergic neurotoxin, reduced the number of TH+ cells in the LC, most significantly on day 10 after injection ($P < 0.0001$, Figure 1I, K) and prolonged the recovery time from midazolam administration ($P < 0.05$, Figure 1G). Moreover, IP injection of DSP-4 for 10 days significantly reversed the recovery-promoting effect of atomoxetine ($P < 0.01$, Figure 1H). These all data suggest that the noradrenergic system participates in midazolam-induced altered consciousness

The activity of LC^{NE} neurons is significantly reduced after midazolam administration

Since LC is the largest nucleus in the brain that syntheses and releases NE, we used fiber photometry to measure the neuronal activity of LC^{NE} neurons at different states after midazolam administration (Figure 2A-B). We injected AAV2/9-DβH-GCaMP6m-WPRE-hGH

pA with a specific promoter into the bilateral LC of C57BL/6J mice to express the GCaMP6m calcium indicator specifically in NEergic neurons and examined changes in GCaMP6m fluorescence signal through an optical fiber located in the LC (Figure 2C). We found that during the LORR to RORR phase, the ΔF/F peak of calcium signaling in LC^{NE} neurons was significantly reduced compared with other phases, and then increased after RORR ($P < 0.05$, $P < 0.01$, Figure 2D-G).

To further evaluate the changes in neuronal activity in the LC after midazolam administration, we performed immunofluorescence staining for c-Fos and TH. Fluorescence images showed a decrease in the number of c-Fos-positive cells co-labeled with TH in the midazolam administration group compared with the control group ($P < 0.01$, Figure 2H-J). These results indicated that LC^{NE} neurons were significantly inhibited after midazolam administration.

LC^{NE} neurons participate in regulating recovery from midazolam

To further explore the role of LC^{NE} neurons in recovery after midazolam administration, we artificially intervened in LC^{NE} neurons. We microinjected DSP-4 into LC to specifically degrade LC^{NE} neurons and found a significant decrease in the number of TH+ neurons in the LC of mice 10 days after the DSP-4 microinjection ($P < 0.0001$, Figure 2O-P). In addition, microinjection of DSP-4 into the LC significantly prolonged the recovery time and attenuated the recovery-promoting effect of IP-injected atomoxetine in midazolam-induced loss of consciousness ($P < 0.05$, Figure 2M-N). These suggest that intranuclear administration of DSP-4 to specifically ablate LC^{NE} neurons suppresses recovery from midazolam administration.

Then, optogenetic manipulation was used to further examine the role of LC^{NE} neurons (Figure 3A-B). For this purpose, we used a Cre-dependent AAV expressing channelrhodopsin-2 (ChR2) fused with enhanced yellow fluorescent protein (AAV-DIO-ChR2–eYFP) and co-infused it with Cre-AAV expressing the TH promoter (TH-Cre-AAV) to restrict the expression of ChR2 to LC TH+ neurons and an optrode was implanted at the injection site (Figure 3C). We found that photostimulation (20 min/4 mW) of LC^{NE} neurons significantly shortened the recovery time and produced a pro-recovery effect from midazolam regardless of whether it was left, right, or bilateral LC optogenetic activation ($P < 0{\cdot}05$, Figure 3D-F). In addition, fluorescence images showed that c-Fos (+)/TH (+) cells were significantly increased after photostimulation of LC^{NE} neurons ($P < 0.0001$, Figure 3G-I).

Next, we tested whether the chemogenetic activation of LC^{NE} neurons promotes recovery (Figure 3J). In order to reveal whether there were sex differences in chemogenetic activation of LC^{NE} neurons, we used both male and female mice, and Cre-dependent excitatory DREADD was co-infused with TH-Cre-AAV to restrict the expression of hM3Dq to LC TH+ neurons (Figure 3K). We determined the transfection efficiency of the chemogenetic virus in LC^{NE} neurons (Figure 3L). Similar results were obtained in the chemogenetic experiment. We found that in both male and female mice ,IP injection of 0.2 mg/kg CNO could shorten the recovery time and produce a pro-recovery effect from midazolam regardless of whether it was left, right, or bilateral LC chemogenetic activation ($P < 0.05$, Figure 3M-P). In addition, c-Fos (+)/TH (+) cells were significantly increased after photostimulation of LC^{NE} neurons ($P < 0.0001$, Figure 3Q-S). Thus far, we have proven that there were no sex differences in

chemogenetic activation of LC^{NE} neurons, and LC^{NE} neurons were involved in the recovery from midazolam.

Activation of the LC-VLPO NEergic neural circuit promotes recovery from midazolam

The LC sends projections to several brain regions, including the VLPO, which is a crucial area in regulating sleep and arousal states. Therefore, we hypothesized that LC and VLPO interact to mediate midazolam-induced alterations in consciousness. To verify the existence of the LC–VLPO projection, we microinjected the mix of mTH-Cre-AAV and AAV-EF1a-DIO-hChR2(H134R)-eYFP viruses into the LC and microinjected rAAV2/9-DβH-GCaMP6m-WPRE-hGH pA into the VLPO, and two weeks later implanted optical fibers into the VLPO to record neuronal firing (Figure 4A-C). We observed local NEergic terminals within the VLPO (Figure 4D, H). Also, we found that optogenetic or chemogenetic activation of LCNE neurons led to an enhanced ΔF/F peak in the VLPO ($P < 0.05$, $P < 0.01$, Figure 4K-T), i.e., increased VLPO activity, as well as facilitated recovery from midazolam ($P < 0.05$, Figure 4E, I-J). Moreover, we found that there were no sex differences in chemogenetics studies.

To further identify whether the LC-VLPO NEergic circuit mediates promoting recovery, we used optogenetics to activate LC^{NE} terminals in the VLPO. We injected the mixture of mTH-Cre-AAV and AAV-EF1a-DIO-hChR2(H134R)-eYFP viruses into bilateral LC and implanted optical fibers above the VLPO (Figure 5A-B). Immunofluorescence results showed co-expression of hChR2 and TH in axon terminals of VLPO after microinjection of hChR2 in the LC (Figure 5D-E). It confirms the structural association between the LC and the VLPO. In addition, the LC-VLPO NEergic terminals were photostimulated with blue light. We found

that the recovery time was shorter in the VLPO photostimulation group than in the no photostimulation group ($P < 0.05$, Figure 5F). Thus, optogenetic activation of VLPO-projecting LCNE neurons promotes recovery from midazolam.

Next, in an attempt to further determine the VLPO-projecting NEergic terminals through which the effects described above are exerted, we combined optogenetic or chemogenetic approaches. Besides, we employed both male and female mice in chemogenetic approach to explore whether there were sex differences. We microinjected the AAV optogenetic or chemogenetic viruses expressing the TH promoter into the VLPO, respectively (Figure 5G-H, L-M). We observed the transfection of the viruses in NEergic axon terminals in the VLPO (Figure 9I-J, N-Q). Moreover, we found that compared with the vehicle, optogenetic and chemogenetic activation of NEergic terminals in the VLPO could reduce the recovery time from midazolam, with no sex difference ($P < 0.05$, Figure 9K, P, R). These suggest that the activation of VLPO-projecting NEergic terminals triggers an immediate pro-recovery effect. Thus far, our results demonstrate the involvement of the LC-VLPO NEergic neural circuit in regulating midazolam-induced altered consciousness.

The promotion of recovery from midazolam is primarily mediated by the α1 adrenergic receptor

To identify the role of different types of noradrenergic receptors in the brain, we used a pharmacological approach. By intracerebroventricular (ICV) injection of different doses of α1-R, α2-R, and β-R agonists and antagonists (Figure 6A), we found that the α1 receptor agonist phenylephrine (20mg/mL) significantly shortened recovery time from midazolam ($P < 0.05$, Figure 6C). Conversely, the α1 receptor antagonist prazosin (1.5mg/mL), the α2 receptor

agonist clonidine (1.5mg/mL), and the β receptor antagonist propranolol (5mg/mL) caused the opposite effects ($P < 0.05$, Figure 6D, E, H). However, the α2 receptor antagonist yohimbine and the β agonist isoprenaline did not affect the recovery time ($P > 0.05$, Figure 6F-G), and phenylephrine significantly reversed the effect of propranolol in prolonging recovery time from midazolam ($P < 0.01$, Figure 6I). These results indicate that the recovery from midazolam is mediated predominantly by α1-R.

The pro-recovery effect of activating LCNE neurons can be reversed by ICV injection or intra-VLPO microinjection of α1-R antagonist

To further determine the link between the LC and VLPO, we assessed the effect of photostimulation and pharmacology (Figure 6J). A mixture of the Cre-dependent AAV vector Ef1a-DIO-hChR2(H134R)-eYFP and mTH-Cre-AAV was injected bilaterally into the LC, and optical fibers were implanted (Figure 6K). 2 weeks later, drug-delivery cannulas were implanted into the ICV or VLPO (Figure 6N, O). Then, we injected prazosin through cannulas within the ICV or VLPO to block α1-R and activate LC by photostimulation to further observe the effects of both on midazolam recovery time. The results showed that photostimulation of LCNE neurons could reduce the recovery time ($P < 0.05$), whereas prazosin could prolong the recovery time ($P < 0.05$), and that prazosin reversed the effects produced by LC activation ($P < 0.01$, $P < 0.001$, Figure 6N, P). Meanwhile, to further assess the effect of the above maneuvers on the depth of sedation, we performed EEG recordings. We found that light stimulation of the LC resulted in some high-amplitude EEG activity and that the use of prazosin caused inhibitory EEG activity (Figure 7A-C), implying that prazosin or LCNE activation may affect the depth of sedation and produce opposite effects.

A similar experiment was performed with the chemogenetic approach (Figure 6Q). The mixture of mTH-Cre-AAV and AAV-Ef1a-DIO-hM3Dq-mCherry viruses was injected into bilateral LC (Figure 6R); 2 weeks later, we determined the transfection efficiency of the chemogenetic virus in LCNE neurons in both male and female mice (Figure 6S, X). For male mice, bilateral drug-delivery cannulas were implanted into the ICV or VLPO (Figure 6T, V); For female mice, bilateral drug-delivery cannulas were implanted into the VLPO (Figure 6Y). α1-R antagonist was microinjected through the cannulas and behavioral tests were conducted as well as EEG recordings. Consistent with the above results, in male mice, both ICV and intra-VLPO injections of prazosin prolonged the recovery time ($P < 0.01$, $P < 0.05$), and reversed the pro-recovery effect produced by chemogenetic activation of LCNE neurons ($P < 0.01$, Figure 6U, W). Also, in female mice, intra-VLPO injections of prazosin prolonged the recovery time ($P < 0.05$), and reversed the pro-recovery effect produced by chemogenetic activation of LCNE neurons ($P < 0.001$, Figure 6Z). Chemogenetic activation of LC leads to some high-amplitude EEG activity, which could be reversed by prazosin (data from male mice, Figure 7D-F).

In sum, the recovery-promoting effects of all the above-mentioned interventions that can activate LCNE neurons can be reversed by prazosin. We also demonstrated the presence of a functional connection between LCNE neurons and VLPO that co-regulates recovery after midazolam, and α1-R on the VLPO is the downstream target involved in the mechanism of recovery from midazolam.

GABAA-R is an important mechanical binding site for midazolam in the LC

Midazolam is a short-acting central benzodiazepine receptor inhibitor that acts primarily on

GABAA-R, thus increasing GABAergic neurotransmission and depressing the CNS. Therefore, we further explored whether LCNE neurons act through GABAA-R after midazolam administration. We microinjected GCaMP6m into the LC in mice and implanted an optical fiber to observe changes in LC calcium signaling after the injection of gabazine, a GABAA receptor antagonist, into the lateral ventricle or LC (Figure 8A). We found that compared with the vehicle, ICV injection and intra-LC microinjection of 4μg/mL gabazine could reduce the recovery time ($P < 0.05$, Figure 8C, E). In addition, gabazine could increase the $\Delta F/F$ peak of calcium signaling in LCNE neurons before LORR and during the RORR to Recovery phase ($P < 0.05$, Figure 4G-J). These data suggest that GABAA-R in LC may be the initiating binding site of midazolam to produce altered consciousness.

We have already demonstrated that midazolam affects LCNE neuronal activity via GABAA-R in the LC, which then exerts its effects via downstream α1-R. First, drug-delivery cannulas were implanted into the LC and VLPO, respectively. One week later gabazine was injected into the LC to block GABAA-R, while prazosin was injected into the VLPO to antagonize α1-R (Figure 8K-L). We found that microinjection of gabazine into the LC could reduce the recovery time ($P < 0.05$), whereas microinjection of prazosin into the VLPO could increase the recovery time ($P < 0.05$, Figure 8N). In addition, we found that microinjection of prazosin into VLPO prolonged the recovery time and significantly reversed the blockade of LC GABAA-R-induced pro-recovery effect ($P < 0.05$, $P < 0.001$, Figure 8N).

To investigate the role of GABAA-R on LCNE neurons in the modulation of recovery from midazolam, we performed a loss-of-function study using shRNA to knockdown GABAA-R in the bilateral LCNE neurons. As assessed by immunofluorescence staining analysis, the

expression of GABAA-R on LCNE neurons was significantly reduced compared to the sham group ($P<0.0001$, Figure 9A-F). We found that knockdown of GABAA-R prolonged the recovery time from midazolam, while did not affect the dose of midazolam-induced LORR ($P<0.01$, Figure 9G-I).

GABA-ergic and NE-ergic systems interact with each other, co-regulate the recovery from midazolam

In previous experiments, we preliminarily proved that GABA-ergic and NE-ergic systems co-regulate recovery from midazolam by the pharmacological method. Then, we combined the gene knockdown technique with fiber photometry to delve deeper (Figure 9J-P). We found that the ΔF/F peak of calcium signaling in the VLPO NE-ergic terminals in the shRNA group was significantly reduced compared with the sham group ($P<0.05$, Figure 9Q-S).

More importantly, we knocked down GABAA-R on LCNE neurons, resulting in fewer targets for midazolam and weakened function of the GABA-ergic system, and similar to previous results, recovery time from midazolam was reduced. Meanwhile, microinjecting NE α1-R antagonist in the VLPO, we found that the reduction of recovery time caused by the knockdown of GABAA-R was reversed ($P<0.05$, Figure 9Y), suggesting that the NE-ergic system is indeed involved in recovery from midazolam with NE α1-R on VLPO neurons is an important functional site in the LC-VLPO neural circuit.

Discussion

Midazolam is of great value in the treatment of psychiatric disorders as sedative-hypnotics. Although the number of clinical studies addressing the effects of midazolam on consciousness as well as behavior is slowly increasing, the specific neural mechanisms by which it alters

consciousness remain unclear. To fill this gap, we chose midazolam, a clinical drug, to study in mice to find a promising target for the development of an effective strategy to provide targeted therapies for the reversal of midazolam-induced delayed recovery.

In the present study, we cascaded our experiments. First, using pharmacology and ELISA, we verified that the central NE system plays an important role in recovery from midazolam sedation. We found that midazolam administration significantly reduced TH activity in the brainstem and that IP injection of atomoxetine, an NE reuptake inhibitor, could shorten recovery time from midazolam, while peripheral injection of DSP-4 reverses the pro-recovery effect of atomoxetine. Second, based on calcium signaling, we found a decrease in LCNE neuronal activity after midazolam administration. Consistent with this, optogenetic and chemogenetic activation of LCNE neurons could facilitate recovery from midazolam, whereas elective ablation of LCNE neurons by intra-LC microinjection of DSP-4 attenuates recovery. Third, we turned our attention to the downstream pathway of the LC. We found that optogenetic and chemogenetic activation of LCNE neurons could influence the activity of VLPO, and ChR2 can be transmitted from the LC to the VLPO across synapses, suggesting that the LC can project to the VLPO. Next, ICV injection of different adrenergic receptor agonists or antagonists suggested the main involvement of α1-R in the regulative effect of recovery from midazolam. Also, we microinjected α1-R antagonist into VLPO, and we found that the pro-arousal effect induced by activation of LCNE neurons was reversed, suggesting that α1-R in the VLPO is more responsive to regulate recovery from midazolam. Then, ICV injection of the GABAA-R antagonist gabazine or microinjection of gabazine into the LC shortened the recovery time from midazolam, and we found that antagonizing GABAA-R

could inhibit the activity of LC, suggesting that GABAA-R in the LC may be an initiating target for the action of midazolam. Finally, by using pharmacological method and gene knockdown technique we found that GABA-ergic and NE-ergic systems co-regulated recovery from midazolam, and GABAA-R on LCNE neurons and NE α1-R on VLPO were the key points. It is worth mentioning that in this study, both male and female mice were used in all chemogenetics experiments, and we found that gender difference did not affect the results of the experiment.

Altered states of consciousness attributed to the action of sedative drugs on molecular targets in the CNS have been the focus of research over the past decades. GABAA-R is a well-recognized target of different sedative agents. GABAA-R is a ligand-gated Cl- channel that mediates the majority of the fast inhibitory neurotransmission in the CNS and has a crucial role in regulating brain excitability. Different GABAA-R subtypes constitute a family of 19 subunit genes, including α1–6, β1–3, γ1–3, δ, ε, θ, π, and ρ1–3, which assemble to form a pentameric structure25. The GABAA-R has a GABA-binding receptor site and some regulatory sites for binding of various substances, and the best characterized regulatory site is the benzodiazepine (BZ) one26. Midazolam is a prevalent psychotropic substance that acts as a positive allosteric modulator of this receptor27. The drug binds highly specifically to the BZ-binding site on the GABAA-R complex, affecting the affinity of GABA and GABA-binding receptor sites and reducing the excitability of the CNS, thus inducing sedation, hypnosis, and unconsciousness. Receptors containing the α1, 2, 3, 5 and γ2 subunit interface form the BZ-binding site of GABAA-R, suggesting the significance of these subunits in midazolam-mediated effects28. It is reported that the duration of the LORR in response to

midazolam was reduced in β3-knockout mice compared with wild-type mice, indicating a role of β3-containing GABAA-R in mediating midazolam-induced unconsciousness29. According to our findings, midazolam modulates downstream neural pathways by initially acting on GABAA-R in the LC. It is future studies of membrane proteins and ion channels in LC or non-LC NEergic neurons that we call for to fully understand the molecular and neural circuit targets of sedative-hypnotics.

Midazolam can induce a state of de-consciousness similar to natural sleep. Its effects may engage endogenous sleep-arousal neural nuclei and circuits to induce hypnosis and loss of consciousness. In conjunction with past studies, midazolam and other sedative drugs act primarily by enhancing GABAergic inhibitory neurotransmission, implying a sleep-like facilitating effect of the GABAergic system. However, the mechanism of neural circuits downstream of GABA that regulate changes in consciousness is unclear.

Arousal in the brain depends on many areas that can simultaneously receive different signals, wherein the ascending reticular activating system (ARAS) is responsible for arousal and controls the maintenance of wakefulness30. LCNE neurons, which are an important component of the ARAS, reportedly play a key role in the maintenance of arousal and alertness31. Specifically, we propose that LCNE neurons and their related circuits are involved in modulating recovery from midazolam. In this study, LCNE neurons were activated by photostimulation and chemogenetics to rapidly induce the transition from unconsciousness to awakening. As a key arousal node, the LC receives inputs from arousal-related neurons and provides widespread NEergic innervation to the cerebral cortex and other forebrain structures32. In our study, we first pharmacologically validated the role of

the central NEergic system in modulating midazolam recovery, and then, since the LC is the predominant nucleus in the brain for the release of NE, we further demonstrated the role of LCNE neurons in midazolam recovery through selective activation and degradation of them. Here, our study elucidates the critical role of NEergic neurons in the LC in midazolam recovery by pharmacology, optogenetics and chemogenetics.

Next, as the VLPO is downstream of the LC and numerous studies have demonstrated its role in integrating information to promote sleep, we spotlighted the LC-VLPO neural circuit. It has been reported that the VLPO contains multiple neuronal populations, including GABAergic and galaninergic neurons, which are considered to be sleep-active neurons33. Interestingly, there is another cluster of glutamatergic neurons in the VLPO that promote arousal34, 35. A recent report showed that LCNE neurons synergistically promote arousal from sleep by simultaneously activating wake-active neurons and inhibiting sleep-active neurons in the VLPO and the regulation of the two types of neurons in the VLPO is mediated by different adrenergic receptors 23. However, our study is quite different from it. First, our study shows that LC may play an irreplaceable role in midazolam-induced loss of consciousness because atomoxetine is a reuptake inhibitor of widespread NE in the brain, but our selective disruption of LC rendered its effect lost. Second, our study revealed that the GABAA-R in the LC may be the key initiating target for midazolam. Third, we identified this α1 receptor as a necessary target through pharmacology and further validated it with more specific means. Finally, we found that intra-VLPO microinjection of the α1 receptor antagonist prazosin significantly reversed the pro-recovery effect of intra-LC microinjection of GABAA receptor antagonist or activation of LCNE neurons. More importantly,

atomoxetine, which is a psychotropic drug commonly used for treating attention-deficit hyperactivity disorder (ADHD), is a promising candidate for translational research to prevent delayed recovery from midazolam abuse in patients with ADHD. Essentially, targeting the central α1-R, particularly in VLPO wake-active neurons, may provide rational therapeutic strategies to prevent delayed recovery. Notably, the VLPO in turn sends GABAergic inhibitory projections to several wake-promoting nuclei throughout the neuroaxis, including the LC36. Several studies have reported that the activated VLPO releases GABA to the LC, thus inducing NREM sleep, and conversely, the NE released from the activated LC inhibits VLPO sleep-active neuron activity and promotes wakefulness37, 38. Therefore, the interactions of the different neuronal populations within the VLPO and their specific connections with the LC in our study need to be further investigated.

The translational implications of a study are a reliable indicator of its impact. The current study has the potential to translate into guidance for the clinical use of midazolam and allow for reducing unwanted drug side effects. On the one hand, we have selected the clinical drug midazolam for animal experiments, which will help us to develop useful drugs to treat midazolam-induced serious complications (e.g., delayed recovery, ventilator-associated pneumonia, and coma) in the future, thus further advancing clinical trials. It provides some hints for management of agitated patients with neuropsychiatric disorders. On the other hand, in addition to intravenous or intramuscular administration, midazolam can also be taken orally to treat insomnia, ameliorate anxiety, and treat seizures and status epilepticus3, 39, 40. Oral midazolam affects consciousness to a greater or lesser extent, and some suicidal patients have even suffered immediate death from massive doses of midazolam. Therefore, our study also

provides clues for medication guidance in such patients.

In summary, our study demonstrates that, in mice, the LC-VLPO NEergic neural circuit mediates rapid modulation of altered consciousness induced by midazolam, which is essential to ameliorate the complications of its abuse. It will pinpoint the relevant regions involved in response to midazolam and provide a perspective to help elucidate the dynamic changes of neural circuits in the brain during altered consciousness, as well as suggest a promising new avenue of investigation for the targets of timely recovery from midazolam-induced loss of consciousness, thereby reducing the threat of delayed recovery and its complications.

Limitations

In our study, we indeed verified that the noradrenergic system plays an important role in modulating midazolam recovery. However, in addition to NE, TH is the rate-limiting enzyme for dopamine synthesis, which has been reported to regulate sleep and arousal. Therefore, we cannot totally exclude a modulatory role of the dopaminergic system on midazolam-induced altered consciousness. Second, our method of labeling NE neurons using wild-type mice in conjunction with a virus-mediated exogenous expression strategy was less specific, and to improve the accuracy of our study, the NE-specific mouse strains can be considered in the future. Furthermore, we will employ more specific tracers to track and investigate the neuronal circuit between LC and VLPO as well as the direct synaptic connections from LCNE neurons to VLPO.

Materials and methods

Ethics

This study was approved by and all experimental procedures were performed in compliance

with the Experimental Animal Ethics Committee of Zhejiang University.

Animals

The experimental animals in this study were male and female wild-type C57BL/6J mice purchased from the Animal Experiment Center of Zhejiang University. All mice were housed and bred in the SPF-Class House in a standard condition (indoor temperature 25°C, ambient humidity 65%, 12-h/12-h light/dark cycle) with rodent food and water available ad libitum. All mice were aged 8 weeks and weighed 22–25 g at the start of the experiments. All experiments were mainly performed between 9:00 and 16:00.

Establishment of a mice model of midazolam administration

We randomly divided healthy C57BL/6J mice into four groups (n = 8). These mice were used to determine the intraperitoneal dose of midazolam that would achieve the optimal depth without inhibiting respiration before starting the formal experiment. Finally, we identified the lowest effective dose that was 100% successful in inducing loss of consciousness in mice, i.e., 60 mg/kg midazolam (H-19990027, Jiangsu Nhwa Pharmaceutical Co., Ltd.), as the optimal dosage for intraperitoneal administration in mice, and used this dose in subsequent experiments.

Evaluation of recovery time

Before the experiment, the bottom of the open box with no lid and air circulation was covered with cotton pads, and an electric blanket was placed on the lower side of the open box, and the temperature in the open box was preheated for 10 min before the experiment to keep the temperature in the open box suitable and constant during the experiment. Eight-week-old C57BL/6J mice were placed in the open box for 30 min, and then placed in the open box

again after intraperitoneal injection of the appropriate dose of midazolam (60 mg/kg) to start the timer. At the same time, the open box was gently rotated every 15 s. When the mice were rotated to the dorsal recumbent position and could not be voluntarily turned over for more than 1 min, it was the loss of righting reflex (LORR), i.e., loss of consciousness from midazolam. Subsequently, the mice were placed in the dorsal recumbent position for continuous observation, and when the mice could autonomously return to the normal position from the dorsal recumbent position, they were considered as recovery of righting reflex (RORR). The time from the onset of LORR to RORR was recorded as the Recovery Time of midazolam.

Enzyme-linked immunosorbent assay (ELISA)

The tyrosine hydroxylase (TH) content and specific enzyme activity were measured in two groups of C57BL/6J mice (n = 6 per group), one group was given 60mg/kg midazolam intraperitoneally and the other group was not. The whole brain was removed and sectioned, and then prosencephalon and brainstem tissue samples were collected separately, and TH levels in these tissues were measured using an enzyme-linked immunosorbent assay (ELISA) kit according to the manufacturer's instructions (YS-M195, YS-M195-1, ELISA Kit, Yan Sheng Biological Technology Co., Ltd., Shanghai, China). The optical density (OD) was measured at 450 nm and 630 nm using an ELISA microplate reader (SynergyMax M5, iD5, Molecular Devices, San Jose, CA, USA).

Stereotaxic surgery and virus microinjection surgery

Eight-week-old C57BL/6J mice were weighed and injected intraperitoneally with 30 mg/kg of pentobarbital, and placed in the rearing cage for about 5~10 min. After complete anesthesia,

the mice were fixed on a stereotactic apparatus (68018, RWD Life Sciences, Shenzhen, China), and the head hairs of the mice were shaved off with a razor. A heating pad was used to maintain the body temperature of mice at 37°C during the procedure, and an ophthalmic ointment was applied to their eyes to avoid dryness. To expose the skull, the scalp was sterilized and a longitudinal incision was made. The periosteum was then removed with 3% hydrogen peroxide and the residue was rinsed with saline. After drilling holes in the skull, the virus was injected into the target site at a flow rate of 40 nL/min via an ultramicro pump (160494 F10E, WPI). We left the needle at the target site for 10 min after injection to allow for diffusion of the virus. To target the LC, the coordinates were AP: −5.41 mm; ML: ±0.9 mm; DV: −3.8 mm. To target the VLPO, the coordinates were AP: −0.01 mm; ML: ±0.65 mm; DV: −5.7 mm. To target the lateral ventricular, the coordinates were AP: −0.47 mm, ML: −1.00 mm, DV: −2.40 mm. According to the experimental needs, optical fibers or catheters were subsequently implanted in the corresponding location and secured with dental cement. After that, the incision was sutured and the mice were placed on a heating blanket to be transferred to a cage when the mice were awake.

Optogenetics

Three weeks before the experiment began, the LC or VLPO was microinjected with an optogenetic virus of 100 nL of a 1:3 volume mixture of mTH-Cre-AAV and AAV-EF1a-DIO-hChR2(H134R)-eYFP (viral titer: 5.00×1012vg/mL, Brain VTA Technology Co., Ltd., Wuhan, China). One week before the experiment began, the LC or VLPO was implanted with optical fibers (FOC-W-1.25-200-0.37-3.0, Inper, Hangzhou, China). TH-hChR2 expression in the LC and VLPO was determined by immunohistochemistry after

the completion of optogenetic experiments. The mice were intraperitoneally injected with midazolam, and 20 min later, they were given 465 nm blue light to activate neurons in the LC or VLPO. In this study, we used different parameters for optogenetic activation: 20 min/2 mW; 20 min/4 mW; 10 min/4 mW; and 20 min/4 mW. We finally identified 20 min/4 mW as the optimal optogenetic activation parameter and used it in the subsequent experiments.

Chemogenetics

Three weeks before starting the experiment, chemogenetic viruses of 100 nL of a 1:3 volume mixture of mTH-Cre-AAV and pAAV-EF1a-DIO-hM3D-mCherry (viral titer: 5.00×1012vg/mL, Brain VTA Technology Co., Ltd., Wuhan, China) were microinjected into the LC or VLPO, and TH-hM3Dq expression in the LC and VLPO was determined by immunohistochemistry after the completion of chemogenetic experiments. Clozapine-N-oxide (CNO) (HY-17366, MedChemExpress) was dissolved in saline, and the mice were intraperitoneally injected with CNO 20 min after intraperitoneally injected with midazolam to activate neurons using the chemogenetics approach. In this study, we tested two concentrations of CNO: 0.1 mg/kg and 0.2 mg/kg. We concluded that 0.2 mg/kg was the optimal concentration and used this concentration for the subsequent intraperitoneal administration.

Fiber photometry

We microinjected 100 nL of rAAV-DβH-GCaMP6m-WPRE-hGH pA (viral titer: 2.00×1012vg/mL, Brain VTA Technology Co., Ltd., Wuhan, China) into the LC or VLPO. Two weeks later, an optical fiber (FOC-W-1.25-200-0.37-3.0, Inper, Hangzhou, China) was implanted in the same area located 0.05 mm above the virus injection point (AP: −5.41 mm;

ML: ±0.9 mm; DV: −3.75 mm/AP: −0.01 mm; ML: ±0.65 mm; DV: −5.65 mm) and fixed in place with dental cement. Three weeks after viral expression and one week after fiber optic placement, the calcium activity of the target neurons was monitored. Fluorescence emissions were recorded using a fiber photometry system (Inper, Hangzhou, China, C11946) using a 488-nm diode laser, and the mice were placed in a dark box to avoid the influence of natural light source on calcium signal recording, and accessed to the computer recording software to record calcium signals. After the recording was completed, the results recorded by the optical fiber were read into the calcium signaling data analysis software. The calcium signalings were recorded 30 min before LORR when the mice were awake. Then, midazolam was injected intraperitoneally. After the RORR, the experiment was terminated after 10 min of optical fiber recording. The calcium signal intensity was calculated as the value of $\Delta F/F=(F-F0)/F0$.

GABAA-R Knockdown

We microinjected 80 nL of rAAV-DBH-EGFP-S'miR-30a-shRNA(GABAA receptor)-3'-miR30a-WPRES (viral titer: 5E+12 vg/mL, Brain VTA Technology Co., Ltd., Wuhan, China) into the LC. Four weeks later, these mice were sacrificed and perfused for counting the GABAA-R (+) and tyrosine hydroxylase-positive (TH+) cells to evaluate the effect of GABAA-R knockdown.

Pharmacological experiments

Effects of intraperitoneal injection of atomoxetine and DSP-4 and their interaction on the recovery time of midazolam

Atomoxetine (Ca #Y0001586, Sigma-Aldrich) which selectively inhibits presynaptic uptake of norepinephrine (NE) and enhances norepinephrine function, was dissolved in saline. One

hour before intraperitoneal injection with midazolam, C57BL/6J mice received intraperitoneal (IP) injection of atomoxetine (10 mg/kg or 20 mg/kg) or saline (vehicle). To evaluate the impact of peripheral injection of atomoxetine on the recovery time of midazolam, three trials were done for each group of mice (vehicle, 10 mg/kg, and 20 mg/kg), and the recovery time was recorded.

To further verify the effect of norepinephrine on the recovery time of midazolam, we used DSP-4 (C8417, Sigma-Aldrich), a selective neurotoxin that targets the LC norepinephrine system in the rodent brain and is used to disrupt nerve terminals and attenuate NE and NE transporter function in the LC-innervated brain regions. We divided the mice into four groups [vehicle + vehicle, vehicle + atomoxetine, DSP-4 (3 d) + atomoxetine, DSP-4 (10 d) + atomoxetine; n = 6 in each group]. The specific experimental method followed was as follows. C57BL/6J mice received intraperitoneal injection of DSP-4 (50 mg/kg) or saline (vehicle) 3 days before or 10 days before the intraperitoneal injection of atomoxetine (20 mg/kg) or saline (vehicle). One hour later, midazolam was intraperitoneally injected, and the recovery time was recorded. Herein, we verified the physiological effects of DSP-4 using immunohistochemistry.

Effect of intra-LC microinjection of DSP-4 and its interaction with intraperitoneal injection of atomoxetine on the recovery time of midazolam

Ten days before the start of this part of the experiment, cannulas were implanted in bilateral LC of C57BL/6J mice using the same method as mentioned above. DSP-4 (200 nL, 10 μg/μL) or saline (vehicle) was injected into the LC through these guide cannulas. After 10 days, the mice were intraperitoneally administered atomoxetine or saline (vehicle) 1 h before the

intraperitoneal injection of midazolam. The recovery time was recorded for vehicle + vehicle, vehicle + atomoxetine, and DSP-4 + atomoxetine groups (n = 6 mice in each group). Using the same protocol as mentioned above, to complete the experiment, the mice were perfused, and their brains were sectioned. Then, the number of TH+ cells in the DSP-4-treated group and vehicle group were counted and compared individually to investigate the effect of DSP-4 microinjection on noradrenergic neurons in bilateral LC.

Effects of lateral ventricle injection and intra-LC microinjection of a GABAA receptor antagonist on the recovery time of midazolam

This experiment was performed in the same batch of 8-week-old C57BL/6J mice 1 week after lateral ventricle cannula and bilateral LC cannula implantation. Three minutes before the intraperitoneal injection of midazolam, 2000 nL of gabazine (2 μg/mL, 4 μg/mL, n = 7, HY-103533, MedChemExpress) was injected into the lateral ventricle cannula or the bilateral cannulas of LC. The recovery time was recorded in each group. During the experiment, the calcium signals were also recorded simultaneously.

Effects of lateral ventricle injection of different adrenoceptor agonists and antagonists on the recovery time of midazolam

The experiment was performed in the same batch of 8-week-old C57BL/6J mice 1 week after lateral ventricle cannula implantation. The mice were administered agonists or antagonists of different adrenergic receptors through the lateral ventricle. Three minutes before intraperitoneal injection of midazolam, 2000 nL of the α1 receptor agonist phenylephrine (10 mg/mL, 20 mg/mL, n = 8, HY-B0471, MedChemExpress) or α1 receptor antagonist prazosin (0.75 mg/mL, 1.5 mg/ml, n = 8, HY-B0193, MedChemExpress) or α2 receptor agonist

clonidine (0.75 mg/mL, 1.5 mg/mL, n = 9, HY-B0409, MedChemExpress) or α2 receptor yohimbine (15 μmol/mL, 22.5 μmol/mL, 30 μmol/mL, n = 8, Y111137, Aladdin) or β receptor agonist isoprenaline (2 mg/mL, 4 mg/mL, n = 7, I5627, Sigma-Aldrich) or β receptor antagonist propranolol (2·5 mg/mL, 5 mg/mL, n = 6, HY-B0573, MedChemExpress) or vehicle was administered via the lateral ventricle catheter. The recovery time was recorded.

To further explore the interaction between the α1 receptor and β receptor, we divided the mice into four groups (vehicle + vehicle, phenylephrine, propranolol, and phenylephrine + propranolol). C57BL/6J mice received intracerebroventricular injection of 2000 nL of phenylephrine (20 mg/kg) or propranolol (5 mg/kg) or phenylephrine (20 mg/kg) + propranolol (5 mg/kg) or vehicle, and 3 min later, they were treated with intraperitoneal injection of midazolam. The recovery time was recorded.

Effects of intra-LC microinjection of GABAA receptor antagonist and intra-VLPO microinjection of α1 receptor antagonist on the recovery time of midazolam

To investigate the interaction between GABAergic and noradrenergic systems, we divided the mice into four groups (vehicle + vehicle, gabazine + vehicle, vehicle + prazosin, and gabazine + prazosin). The experiment was performed 1 week after LC or VLPO cannula implantation. 200 nL of Gabazine, prazosin, or vehicle in the same volume was microinjected into the LC or VLPO through the guide cannula. Three minutes later, the mice were intraperitoneally injected with midazolam. The recovery time was recorded.

EEG recording and analysis

Mice with 2 weeks of viral infection in the target brain area were anesthetized with intraperitoneal injection of 30 mg/kg pentobarbital and fixed on a stereotaxic apparatus to

expose the skull for leveling. The top of the head was shaved for all mice, and then the skin was sterilized and dissected to expose the skull. Then, four screws with wires were drilled in the left and right of the fontanelle and in the left and right anterior of the posterior fontanelle, and these were then connected to the headstage where the electroencephalogram (EEG) was recorded. This was followed by dental bone cement stabilization and the application of erythromycin ointment to the operative region. Mice equipped with an EEG headstage were housed individually for one week until they adapted to the recording cable and then moved to the experimental barrel, and the EEG activity of the mice was recorded using the EEG monitor and software.

Immunohistochemistry

For immunohistochemistry analysis of the brain, the mice were euthanized after the experiments, and their brains were carefully extracted from the skull. After perfusion with 4% paraformaldehyde (PFA) in phosphate-buffered saline (PBS), the brains were saturated in 30% sucrose for 24 h. Then, coronal slices (thickness, 35 μm) were cut using a freezing microtome (CM30503, Leica Biosystems, Buffalo Grove, IL, USA). Frozen slices were washed three times in PBS for 5 min and incubated in a blocking solution containing 10% normal donkey serum (017-000-121, Jackson Immuno Research, West Grove, PA), 1% bovine serum albumin (A2153, Sigma-Aldrich), and 0·3% Triton X-100 in PBS for 2 h at room temperature. The sections were incubated with primary antibodies at 4°C overnight; this was followed by incubation in a solution of secondary antibodies for 2 h at room temperature. The primary antibodies used were rabbit anti-TH (1:1000; AB152, Merck-Millipore), mouse anti-TH (1:1000; MAB318, Merck-Millipore), Mouse anti-GABAA-R(1:500; ab94585,

Abcam), and rabbit anti-c-Fos (1:1000, 2250T Rabbit mAb, Cell Signaling Technology, Danvers, Massachusetts, USA), and the secondary antibodies used were donkey anti-rabbit Alexa 546 (1:1000; A10040, Thermo Fisher Scientific), donkey anti-mouse Alexa 546 (1:1000; A10036, Thermo Fisher Scientific), Goat anti-rabbit Cy5 (1:1000; A10523, Thermo Fisher Scientific), donkey anti-rabbit Alexa 488 (1:1000; A21206, Thermo Fisher Scientific), and donkey anti-mouse Alexa 488 (1:1000; A21202, Thermo Fisher Scientific). The brain slices were washed three times with PBS for 15 min, and then, they were deposited on glass slides and incubated in a DAPI solution at room temperature for 7 min. Finally, an anti-fluorescence attenuating tablet was applied to seal the slides. Confocal images were acquired using a Nikon A1 laser-scanning confocal microscope (Nikon, Tokyo, Japan), and further image processing was done using ImageJ (NIH, Baltimore, MD).

Statistical analysis

All the experimental data were reported as mean ± SD. GraphPad Prism (GraphPad Software, Inc., San Diego, CA, USA) and SPSS (SPSS Software Inc., Chicago, IL, USA) were used for data visualization and statistical analysis, respectively. Before data analysis, all experimental data were subjected to the Shapiro-Wilk normality test. For comparative analyses of the two groups, if the data were normally distributed, Student's t-test, including independent samples t-test and paired samples t-test, was used. Conversely, if the data were non-normally distributed, the Mann–Whitney U test or Wilcoxon signed-rank test was used. Notably, the Levene test was used to evaluate the homogeneity of variances. After the data met the normal distribution and homogeneity of variances, a one-way analysis of variance followed by Bonferroni's multiple comparison test was used for multiple comparisons. $P < 0.05$ indicated

statistical significance.

Author contributions

HHZ designed the study. LYG, WHS, QX and YLW performed and analyzed most of the experiments. LL, JXG, QY and XTL helped with the analysis of experiments. We are grateful to YuDong Zhou and Yi Shen for the experimental design.

Acknowledgments

The work was supported by the National Natural Science Foundation of China (Grant no: 81771403, 81974205), the Natural Science Foundation of Zhejiang Province (LZ20H090001), and the Program of New Century 131 outstanding young talent plan top-level of Hang Zhou to HHZ. We thank YuDong Zhou and Yi Shen for their help in experimental design.

Conflict of interest

The authors declare no conflicts of interest.

Data availability

The data supporting the findings of this study are available within the article upon reasonable request.

References

1. Reves JG, Fragen RJ, Vinik HR, Greenblatt DJ. Midazolam: pharmacology and uses. Anesthesiology 1985; 62(3): 310-324.

2. Mandrioli R, Mercolini L, Raggi MA. Benzodiazepine metabolism: an analytical

perspective. Current drug metabolism 2008; 9(8): 827-844.

3. Conway A, Rolley J, Sutherland JR. Midazolam for sedation before procedures. The Cochrane database of systematic reviews 2016; 2016(5): Cd009491.

4. Perlis ML, Posner D, Riemann D, Bastien CH, Teel J, Thase M. Insomnia. Lancet (London, England) 2022; 400(10357): 1047-1060.

5. Sutton EL. Insomnia. Annals of internal medicine 2021; 174(3): Itc33-itc48.

6. Buysse DJ. Insomnia. Jama 2013; 309(7): 706-716.

7. Gebara MA, Siripong N, DiNapoli EA, Maree RD, Germain A, Reynolds CF et al. Effect of insomnia treatments on depression: A systematic review and meta-analysis. Depression and anxiety 2018; 35(8): 717-731.

8. Riemann D, Nissen C, Palagini L, Otte A, Perlis ML, Spiegelhalder K. The neurobiology, investigation, and treatment of chronic insomnia. The Lancet Neurology 2015; 14(5): 547-558.

9. Citrome L. Agitation in schizophrenia: origins and evidence-based treatment. Current opinion in psychiatry 2021; 34(3): 216-221.

10. Kim HK, Leonard JB, Corwell BN, Connors NJ. Safety and efficacy of pharmacologic agents used for rapid tranquilization of emergency department patients with acute agitation or excited delirium. Expert opinion on drug safety 2021; 20(2): 123-138.

11. Shafer A. Complications of sedation with midazolam in the intensive care unit and a comparison with other sedative regimens. Critical care medicine 1998; 26(5): 947-956.

12. Kanto JH. Midazolam: the first water-soluble benzodiazepine. Pharmacology, pharmacokinetics and efficacy in insomnia and anesthesia. Pharmacotherapy 1985; 5(3): 138-155.

13. Olkkola KT, Ahonen J. Midazolam and other benzodiazepines. Handbook of experimental pharmacology 2008; (182): 335-360.

14. Shehabi Y, Bellomo R, Reade MC, Bailey M, Bass F, Howe B et al. Early intensive care sedation predicts long-term mortality in ventilated critically ill patients. American journal of respiratory and critical care medicine 2012; 186(8): 724-731.

15. Massimini M, Ferrarelli F, Sarasso S, Tononi G. Cortical mechanisms of loss of consciousness: insight from TMS/EEG studies. Archives italiennes de biologie 2012; 150(2-3): 44-55.

16. Benarroch EE. Locus coeruleus. Cell and tissue research 2018; 373(1): 221-232.

17. Poe GR, Foote S, Eschenko O, Johansen JP, Bouret S, Aston-Jones G et al. Locus coeruleus: a new look at the blue spot. Nature reviews Neuroscience 2020; 21(11): 644-659.

18. Suárez-Pereira I, Llorca-Torralba M, Bravo L, Camarena-Delgado C, Soriano-Mas C, Berrocoso E. The Role of the Locus Coeruleus in Pain and Associated Stress-Related Disorders. Biological psychiatry 2022; 91(9): 786-797.

19. Carter ME, Yizhar O, Chikahisa S, Nguyen H, Adamantidis A, Nishino S et al. Tuning arousal with optogenetic modulation of locus coeruleus neurons. Nature neuroscience 2010; 13(12): 1526-1533.

20. Chou TC, Bjorkum AA, Gaus SE, Lu J, Scammell TE, Saper CB. Afferents to the ventrolateral preoptic nucleus. The Journal of neuroscience : the official journal of the Society for Neuroscience 2002; 22(3): 977-990.

21. Sherin JE, Shiromani PJ, McCarley RW, Saper CB. Activation of ventrolateral preoptic neurons during sleep. Science (New York, NY) 1996; 271(5246): 216-219.

22. Sherin JE, Elmquist JK, Torrealba F, Saper CB. Innervation of histaminergic

tuberomammillary neurons by GABAergic and galaninergic neurons in the ventrolateral preoptic nucleus of the rat. The Journal of neuroscience : the official journal of the Society for Neuroscience 1998; 18(12): 4705-4721.

23. Liang Y, Shi W, Xiang A, Hu D, Wang L, Zhang L. The NAergic locus coeruleus-ventrolateral preoptic area neural circuit mediates rapid arousal from sleep. Current biology : CB 2021; 31(17): 3729-3742.e3725.

24. Nelson LE, Lu J, Guo T, Saper CB, Franks NP, Maze M. The alpha2-adrenoceptor agonist dexmedetomidine converges on an endogenous sleep-promoting pathway to exert its sedative effects. Anesthesiology 2003; 98(2): 428-436.

25. Ghit A, Assal D, Al-Shami AS, Hussein DEE. GABA(A) receptors: structure, function, pharmacology, and related disorders. Journal, genetic engineering & biotechnology 2021; 19(1): 123.

26. Sigel E, Ernst M. The Benzodiazepine Binding Sites of GABA(A) Receptors. Trends in pharmacological sciences 2018; 39(7): 659-671.

27. Olsen RW. GABA(A) receptor: Positive and negative allosteric modulators. Neuropharmacology 2018; 136(Pt A): 10-22.

28. Maramai S, Benchekroun M, Ward SE, Atack JR. Subtype Selective γ-Aminobutyric Acid Type A Receptor (GABA(A)R) Modulators Acting at the Benzodiazepine Binding Site: An Update. Journal of medicinal chemistry 2020; 63(7): 3425-3446.

29. Quinlan JJ, Homanics GE, Firestone LL. Anesthesia sensitivity in mice that lack the beta3 subunit of the gamma-aminobutyric acid type A receptor. Anesthesiology 1998; 88(3): 775-780.

30. Lee SH, Dan Y. Neuromodulation of brain states. Neuron 2012; 76(1): 209-222.

31. Berridge CW, Schmeichel BE, España RA. Noradrenergic modulation of wakefulness/arousal. Sleep medicine reviews 2012; 16(2): 187-197.

32. Hayat H, Regev N, Matosevich N, Sales A, Paredes-Rodriguez E, Krom AJ et al. Locus coeruleus norepinephrine activity mediates sensory-evoked awakenings from sleep. Science advances 2020; 6(15): eaaz4232.

33. Arrigoni E, Fuller PM. The Sleep-Promoting Ventrolateral Preoptic Nucleus: What Have We Learned over the Past 25 Years? International journal of molecular sciences 2022; 23(6).

34. Chung S, Weber F, Zhong P, Tan CL, Nguyen TN, Beier KT et al. Identification of preoptic sleep neurons using retrograde labelling and gene profiling. Nature 2017; 545(7655):

477-481.

35. Vanini G, Bassana M, Mast M, Mondino A, Cerda I, Phyle M et al. Activation of Preoptic GABAergic or Glutamatergic Neurons Modulates Sleep-Wake Architecture, but Not Anesthetic State Transitions. Current biology : CB 2020; 30(5): 779-787.e774.

36. Saper CB, Scammell TE, Lu J. Hypothalamic regulation of sleep and circadian rhythms. Nature 2005; 437(7063): 1257-1263.

37. Brown RE, Basheer R, McKenna JT, Strecker RE, McCarley RW. Control of sleep and wakefulness. Physiological reviews 2012; 92(3): 1087-1187.

38. Van Egroo M, Koshmanova E, Vandewalle G, Jacobs HIL. Importance of the locus coeruleus-norepinephrine system in sleep-wake regulation: Implications for aging and Alzheimer's disease. Sleep medicine reviews 2022; 62: 101592.

39. Nordt SP, Clark RF. Midazolam: a review of therapeutic uses and toxicity. The Journal of emergency medicine 1997; 15(3): 357-365.

40. Smith R, Brown J. Midazolam for status epilepticus. Australian prescriber 2017; 40(1): 23-25.

1 FIGURE LEGENDS

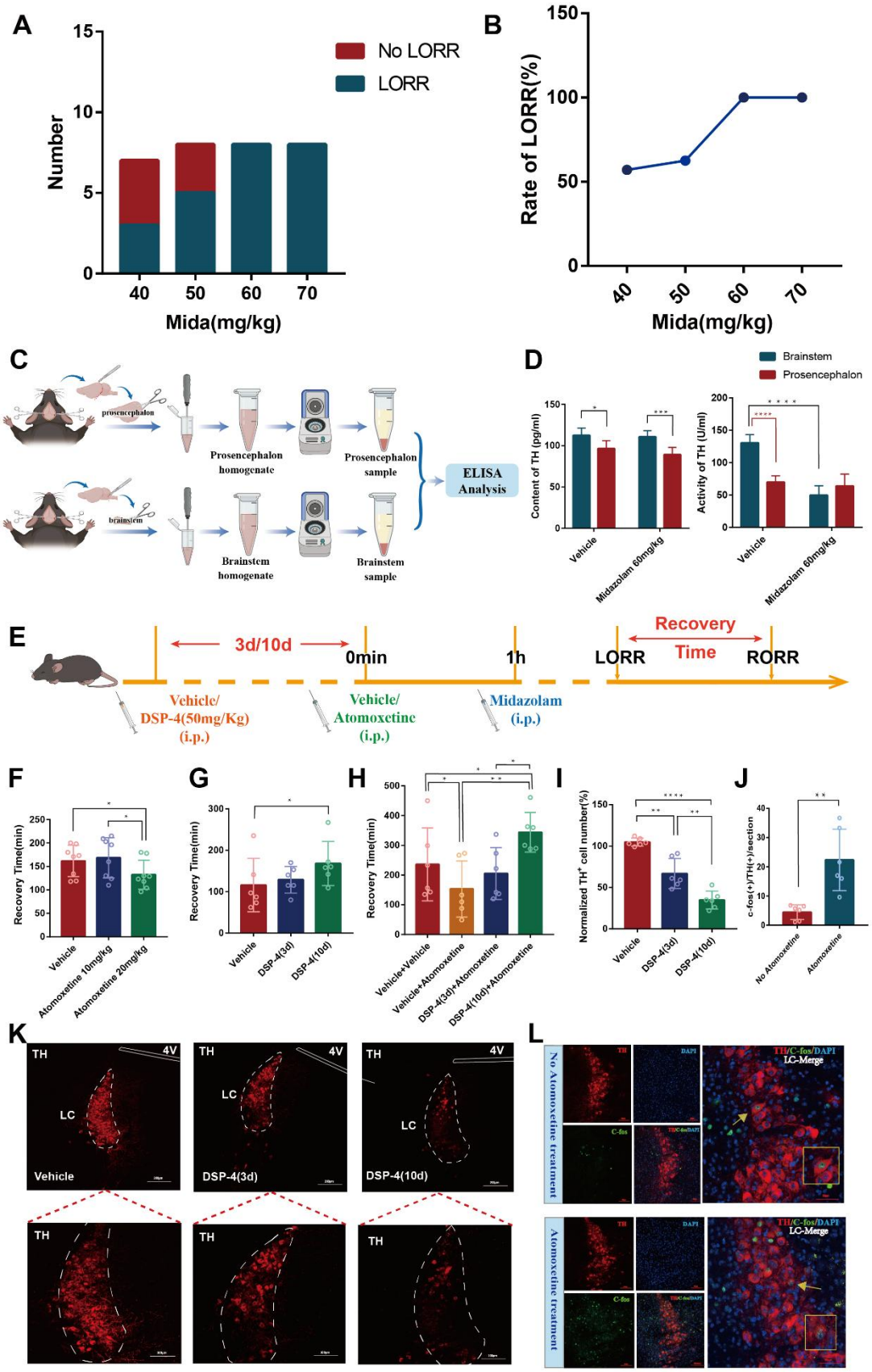

2

Figure 1. The noradrenergic system is involved in recovery from midazolam administration.

(A) Number of LORR and no LORR induced by different doses of midazolam in C57BL/6J mice.

(B) Rate of LORR (%) in C57BL/6J mice at different doses of midazolam.

(C) Protocol for investigating changes in the content and activity of TH in the prosencephalon and brainstem of C57BL/6J mice by ELISA.

(D) Left: Content of TH in the prosencephalon and brainstem in the vehicle and midazolam (60mg/Kg, i.p.) groups. Right: Activity of TH in the prosencephalon and brainstem in the vehicle and midazolam (60mg/Kg, i.p.) groups.

(E) Protocol for exploring the influence of intraperitoneal injection of DSP-4 on the atomoxetine-mediated shortening of the recovery time from midazolam administration.

(F) Comparison of recovery time in the vehicle, Atomoxitine (10mg/Kg, i.p.), and Atomoxitine (20mg/Kg, i.p.) groups.

(G) Comparison of recovery time in the vehicle, DSP-4 (50 mg/kg, 3 days before, i.p.), and DSP-4 (50 mg/kg, 10 days before, i.p.) groups.

(H) Comparison of recovery time in the vehicle + vehicle, vehicle + Atomoxitine, DSP-4 (3 days before) + Atomoxitine, and DSP-4(10 days before) + Atomoxitine groups.

(I) Comparison of normalized TH (+) cell number in the LC in the vehicle, DSP-4 (3 days before), and DSP-4(10 days before).

(J) The quantification of c-Fos (+)/TH (+) cells with or without intraperitoneal injection of atomoxetine.

(K) Images of TH+ neurons in the LC after intraperitoneal injection of vehicle, DSP-4 (3

days), or DSP-4 (10 days) (panels on the lower show magnified images of the panels on the upper).

(L) Representative images showing the changes in TH (+) neuronal activity with or without intraperitoneal injection of atomoxetine.

Mida: midazolam; TH: Tyrosine hydroxylase; *$p<0.05$; **$p<0.01$; ***$p<0.001$; ****$p<0.0001$

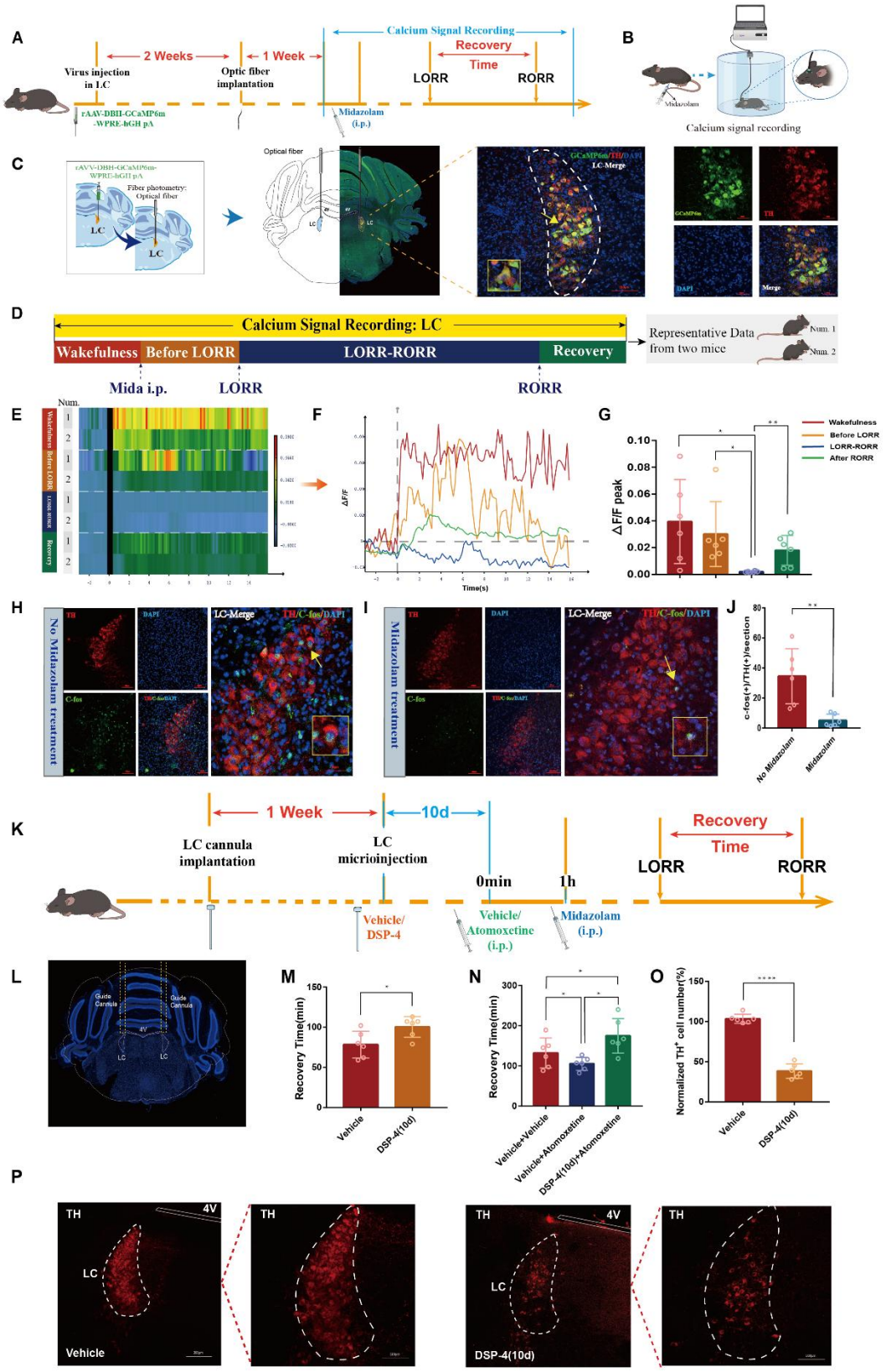

Figure 2. LCNE neuronal activity is significantly reduced after midazolam administration and selective ablation of LCNE neurons hinders recovery from midazolam

(A) A schematic of the fiber optic recording of calcium signalings in the LC.

(B) A schematic of the calcium signaling recording device.

(C) A representative photomicrograph showing the microinjection and optical fiber locations and the co-expression of GCaMP6s and TH.

(D) Schematic diagram of the method of dividing the entire recording of the calcium signal at the BLA into four stages, and sources of heatmap and ΔF/F(%) statistical data.

(E) A heatmap of calcium signaling changes in bilateral LCNE neurons induced by midazolam. (Two representative mice were selected for the fiber optic recording of calcium signals, and the whole recording was divided into four stages, each stage as a group for statistical analysis of calcium signaling).

(F) A statistical diagram of calcium signaling changes in bilateral LCNE neurons induced by midazolam.

(G) The peak ΔF/F in the wakefulness, before LORR, LORR-RORR, and after RORR stages.

(H-I) Representative images showing the co-expression of c-Fos and TH in the LC without or with midazolam treatment.

(J) The quantification of c-Fos (+)/TH (+) cells in the LC with midazolam or without midazolam treatment.

(K) Protocol for exploring the influence of intra-LC microinjection DSP-4 on the atomoxetine-mediated shortening of the recovery time from midazolam administration.

(L) The representative photomicrograph shows the tracks of cannulas implanted into bilateral LC.

(M) Results showed the effects of microinjection of DSP-4 (10 days before) into bilateral LC

on the recovery time of midazolam.

(N) Results showed the effects of vehicle + vehicle, vehicle + atomoxetine, and DSP-4 (10 days before) + atomoxetine on the recovery time of midazolam.

(O) Comparison of normalized TH (+) cell number in the LC with or without DSP-4 (10 days before) microinjected in the bilateral LC.

(P) Images of TH+ neurons in the LC after microinjection of DSP-4 or vehicle for 10 days (panels on the right show magnified images of the panels on the left).

*$p<0.05$; **$p<0.01$; ****$p<0.0001$

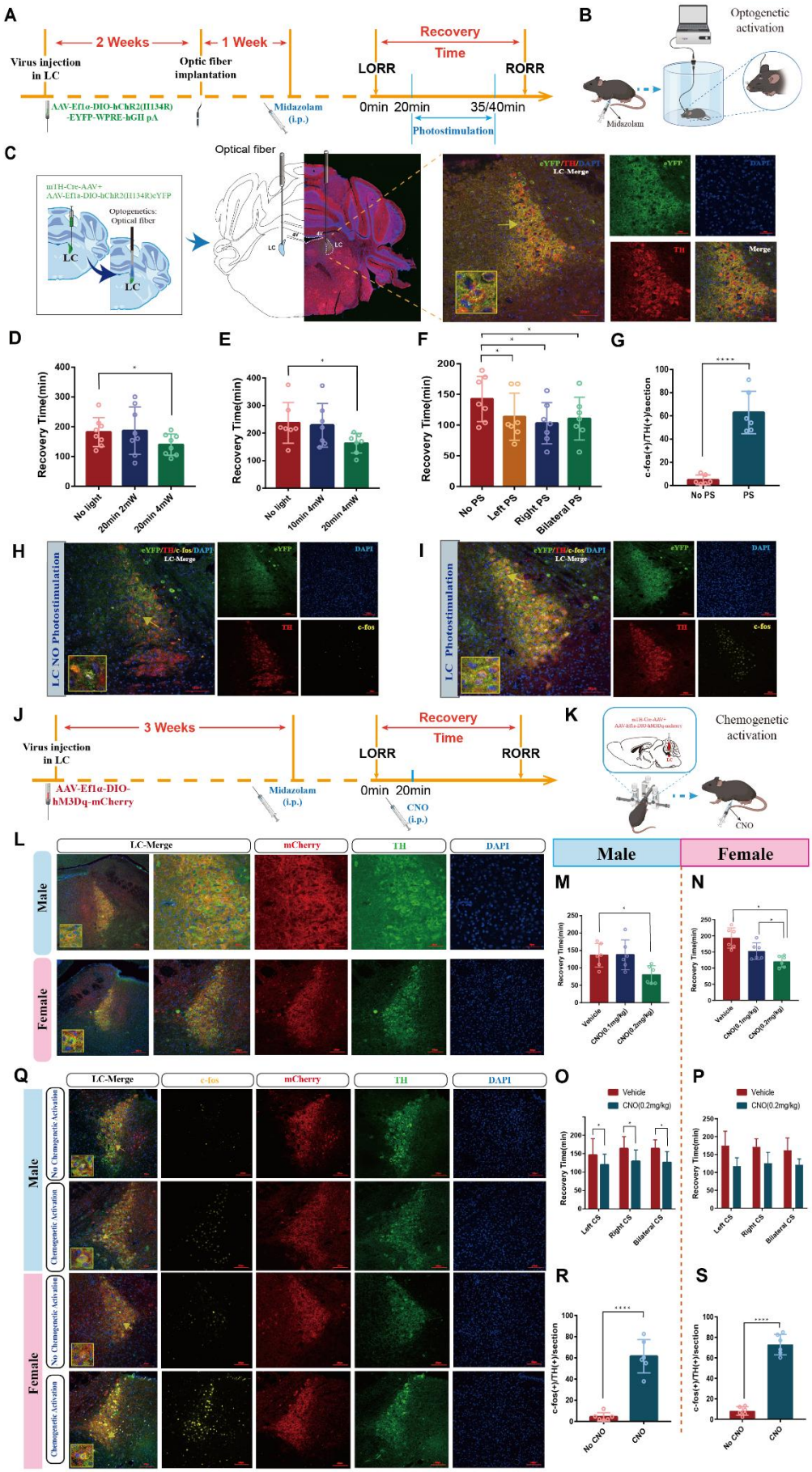
A
2 Weeks
1 Week
Virus injection in LC
Optic fiber implantation
AAV-Ef1α-DIO-hChR2(H134R)-EYFP-WPRE-hGH pA
Midazolam (i.p.)
Recovery Time
LORR
RORR
0min 20min
35/40min
Photostimulation
B
Optogenetic activation
Midazolam
C
Optical fiber
m1H-Cre-AAV+ AAV-Ef1a-DIO-hChR2(H134R)eYFP
Optogenetics: Optical fiber
LC
eYFP/TH/DAPI
LC-Merge
eYFP
DAPI
TH
Merge
D
Recovery Time(min)
No light
20min 2mW
20min 4mW
E
No light
10min 4mW
20min 4mW
F
No PS
Left PS
Right PS
Bilateral PS
G
c-fos(+)/TH(+)section
No PS
PS
H
LC NO Photostimulation
eYFP/TH/c-fos/DAPI
c-fos
I
LC Photostimulation
J
3 Weeks
Virus injection in LC
AAV-Ef1α-DIO-hM3Dq-mCherry
Midazolam (i.p.)
0min 20min
CNO (i.p.)
K
Chemogenetic activation
CNO
L
LC-Merge
mCherry
TH
DAPI
Male
Female
M
Vehicle
CNO(0.1mg/kg)
CNO(0.2mg/kg)
N
Q
c-fos
No Chemogenetic Activation
Chemogenetic Activation
O
CNO(0.2mg/kg)
Left CS
Right CS
Bilateral CS
P
R
No CNO
CNO
S

Figure 3. Optogenetic or chemogentic activation of LCNE neurons promotes recovery from midazolam

(A) Protocol for the effect of photostimulation of LCNE neurons with different light parameters on the recovery time of midazolam.

(B) A schematic of the photogenetic instrument.

(C) A representative photomicrograph showing the locations of optical fiber and virus expression and the co-expression of hChR2 and TH.

(D-E) Results showed the effect of photostimulation of LCNE neurons with different light parameters on the recovery time of midazolam.

(F) Results showed the effect of left, right, and bilateral photostimulation of the LCNE neurons on the recovery time of midazolam.

(G) The quantification of c-Fos (+)/TH (+) cells in the LC with or without photostimulation.

(H-I) Representative images showing the co-expression of c-Fos and TH cells in the LC with or without photostimulation.

(J-K) Protocol and instrument for the effect of chemogenetic activation of LCNE neurons on the recovery time of midazolam.

(L) A representative photomicrograph showing the virus expression and the co-expression of mCherry and TH in the LC of male and female mice.

(M-N) Results showed the effect of chemogenetic activation of LCNE neurons with different doses of CNO (i.p.) on the recovery time of midazolam in male and female mice.

(O-P) Results showed the effect of left, right, and bilateral chemogenetic activation of the LCNE neurons on the recovery time of midazolam in male and female mice.

(Q) Representative images showing the co-expression of c-Fos and TH cells in the LC of male and female mice with or without intraperitoneal injection of CNO (0.2 mg/kg).

(R-S) The quantification of c-Fos (+)/TH (+) cells in the LC with or without chemogenetic stimulation.

PS: photostimulation; CS: chemogenetic stimulation; *$p<0.05$; ****$p<0.0001$

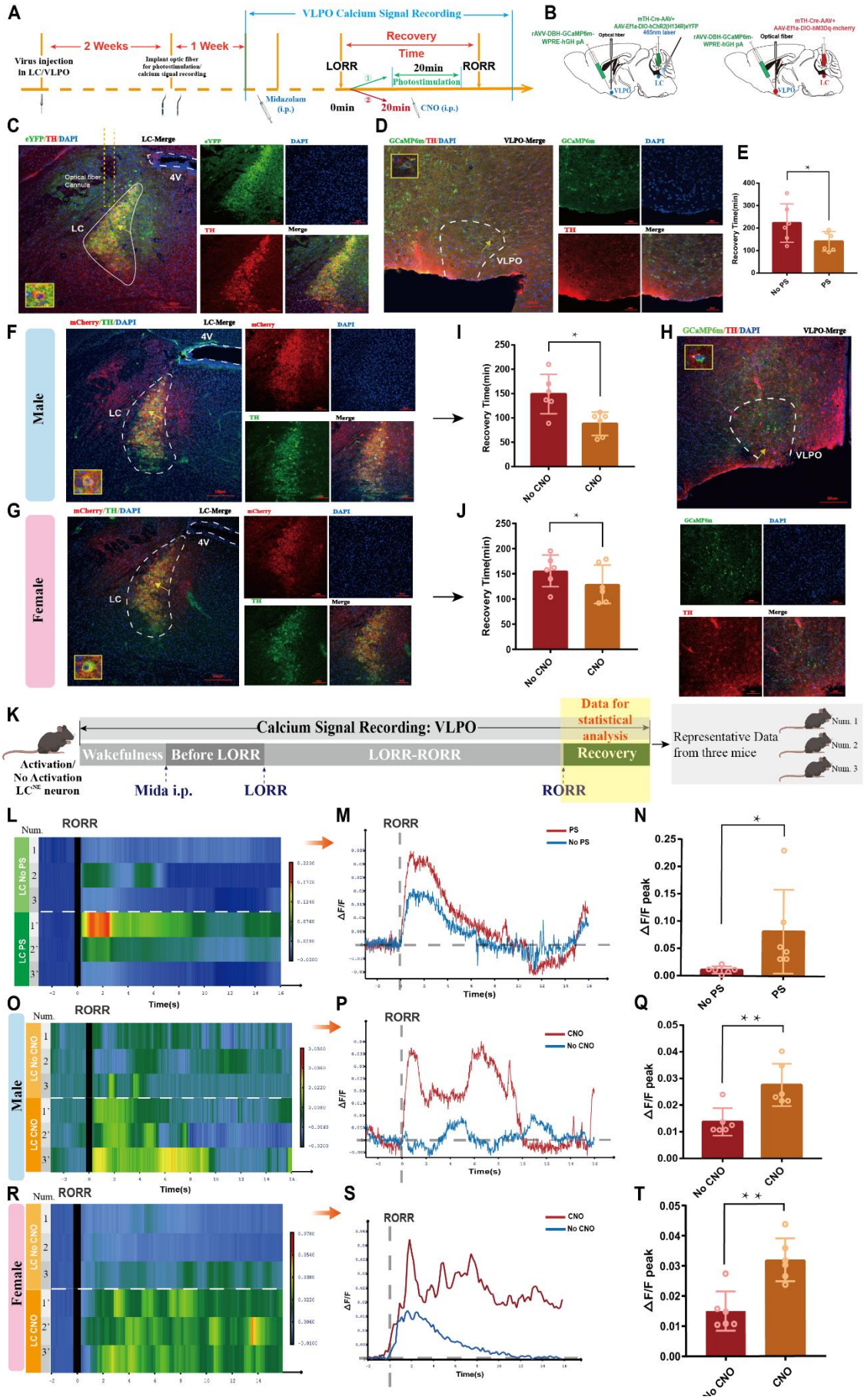
A
VLPO Calcium Signal Recording
2 Weeks
1 Week
Virus injection in LC/VLPO
Implant optic fiber for photostimulation/ calcium signal recording
Recovery Time
LORR
RORR
20min
Photostimulation
Midazolam (i.p.)
0min
20min
CNO (i.p.)
B
C
D
E
F
Male
G
Female
H
I
J
K
Calcium Signal Recording: VLPO
Data for statistical analysis
Wakefulness
Before LORR
LORR-RORR
Recovery
Activation/ No Activation LC^NE neuron
Mida i.p.
LORR
RORR
Representative Data from three mice
Num. 1
Num. 2
Num. 3
L
M
N
O
P
Q
R
S
T
RORR
Time(s)
ΔF/F
ΔF/F peak
PS
No PS
CNO
No CNO
LC No PS
LC PS
LC No CNO
LC CNO
Recovery Time(min)

Figure 4. LC-VLPO NEergic neural circuit was involved in the recovery from midazolam

(A) Protocol for optogenetic or chemogenetic activation of LCNE neurons and recording of calcium signaling changes in VLPO.

(B) A schematic of the location of optogenetic or chemogenetic virus injection site in the LC and calcium signaling recording virus injection site in the VLPO.

(C) A representative image showing the co-expression of hChR2 and TH in the LC.

(D) A representative image showing the co-expression of GCaMP6s and TH in the VLPO in male mice.

(E) Results showed the effects of optogenetic activation of LCNE neurons on the recovery time of midazolam.

(F-G) A representative image showing the co-expression of hM3Dq and TH in the LC of male and female mice.

(H) A representative image showing the co-expression of GCaMP6s and TH in the VLPO in female mice.

(I-J) Results showed the effects of chemogenetic activation of LCNE neurons on the recovery time of midazolam in male and female mice.

(K) Schematic diagram of the method of recording the calcium signal at the VLPO, and sources of statistical data.

(L-M) Heatmap and statistical diagram of calcium signaling changes in bilateral VLPO at the after RORR stage with or without optogenetic activation of LCNE neurons. (Showing changes in calcium signaling during the RORR and the Recovery period; optogenetic activation group, n=3; no optogenetic activation group, n=3)

(N) The peak ΔF/F in the VLPO with or without activation of LCNE neurons using optogenetics.

(O-P, R-S) Heatmap and statistical diagram of calcium signaling changes in bilateral VLPO at the after RORR stage with or without chemogenetic activation of LCNE neurons in male and female mice. (Showing changes in calcium signaling during the RORR and the Recovery period; chemogenetic activation group, n=3; no chemogenetic activation group, n=3)

(Q, T) The peak ΔF/F in the VLPO with or without activation of LCNE neurons using chemogenetics in male and female mice.

PS: photostimulation; *p<0.05; **p<0. 01

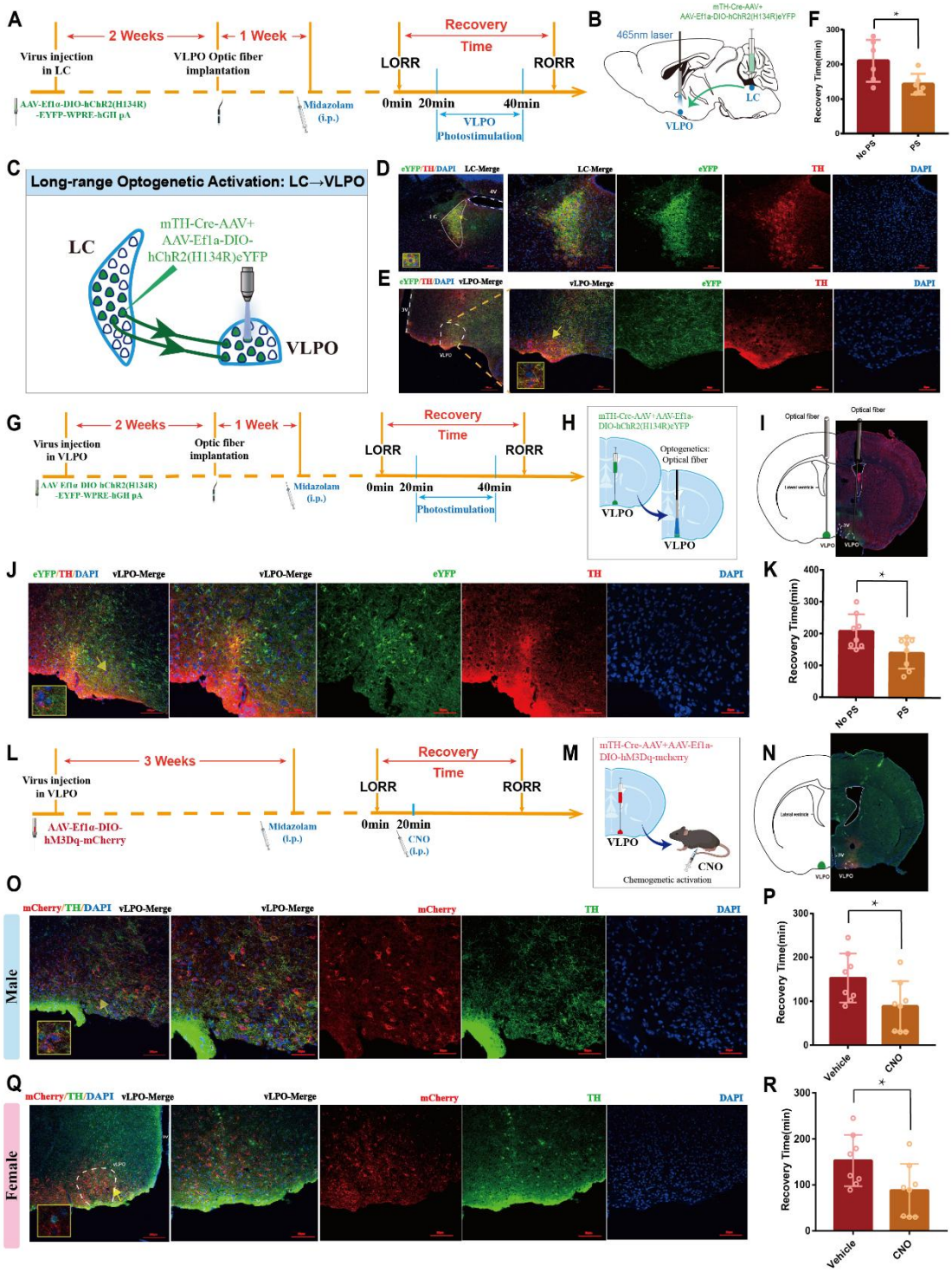

Figure 5. Activation of LC-VLPO NEergic neural circuit promotes recovery from midazolam

(A) Protocol for intra-LC microinjection of the virus and optogenetic activation of VLPO.

(B-C) Schematic of LC–VLPO long-range optogenetic activation and the location of optogenetic virus microinjection and optic fiber implantation.

(D-E) Representative images showing the co-expression of hChR2 and TH in the LC and VLPO.

(F) Result showed the effect of LC–VLPO long-range optogenetic activation on the recovery time of midazolam.

(G, L) Protocols for exploring the influence of optogenetic or chemogentic activation of NEergic terminals in the VLPO on the recovery time from midazolam.

(H, M) Schematic of the brief process of optogenetic or chemogenetic activation.

(I, N) Schematic of the location of optogenetic or chemogenetic virus microinjection and the location of optic fiber implantation.

(J) A representative photomicrograph showing the co-expression of eYFP and TH in the VLPO.

(K) Results showed the effect of Optogenetic activation of NEergic terminals in the VLPO could reduce the recovery time from midazolam.

(O, Q) A representative photomicrograph showing the co-expression of hM3Dq and TH in the VLPO.

(P, R) Results showed the effect of chemogenetic activation of NEergic terminals in the VLPO could reduce the recovery time from midazolam in both male and female mice.

PS: photostimulation; *$p<0.05$

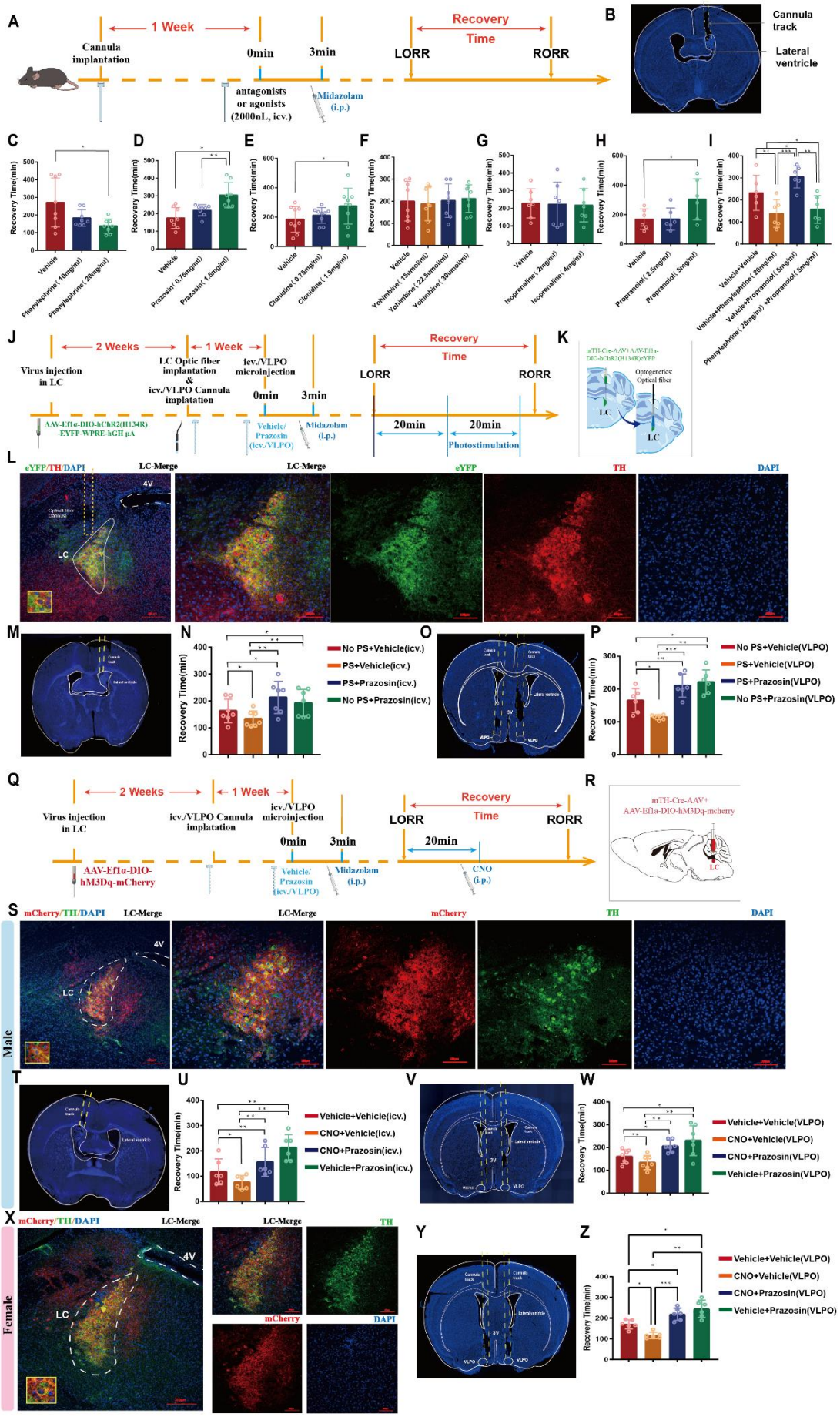
A
1 Week
Cannula implantation
0min
3min
Recovery Time
LORR
RORR
antagonists or agonists (2000nL, icv.)
Midazolam (i.p.)
B
Cannula track
Lateral ventricle
C
D
E
F
G
H
I
Recovery Time(min)
Vehicle
Phenylephrine (10mg/ml)
Phenylephrine (20mg/ml)
Prazosin (0.75mg/ml)
Prazosin (1.5mg/ml)
Clonidine (0.75mg/ml)
Clonidine (1.5mg/ml)
Yohimbine (15umol/ml)
Yohimbine (22.5umol/ml)
Yohimbine (30umol/ml)
Isoprenaline (2mg/ml)
Isoprenaline (4mg/ml)
Propranolol (2.5mg/ml)
Propranolol (5mg/ml)
Vehicle+Vehicle
Vehicle+Phenylephrine (20mg/ml)
Vehicle+Propranolol (5mg/ml)
Phenylephrine (20mg/ml) +Propranolol (5mg/ml)
J
2 Weeks
1 Week
Virus injection in LC
LC Optic fiber implantation & icv./VLPO Cannula implatation
icv./VLPO microinjection
0min
3min
Recovery Time
LORR
RORR
AAV-Ef1α-DIO-hChR2(H134R)-EYFP-WPRE-hGH pA
Vehicle/ Prazosin (icv./VLPO)
Midazolam (i.p.)
20min
20min
Photostimulation
K
mTH-Cre-AAV+AAV-Ef1a-DIO-hChR2(H134R)eYFP
Optogenetics: Optical fiber
LC
L
eYFP/TH/DAPI
LC-Merge
eYFP
TH
DAPI
4V
LC
M
N
O
P
No PS+Vehicle(icv.)
PS+Vehicle(icv.)
PS+Prazosin(icv.)
No PS+Prazosin(icv.)
No PS+Vehicle(VLPO)
PS+Vehicle(VLPO)
PS+Prazosin(VLPO)
No PS+Prazosin(VLPO)
Q
2 Weeks
1 Week
Virus injection in LC
icv./VLPO Cannula implatation
icv./VLPO microinjection
0min
3min
Recovery Time
LORR
RORR
20min
AAV-Ef1α-DIO-hM3Dq-mCherry
Vehicle/ Prazosin (icv./VLPO)
Midazolam (i.p.)
CNO (i.p.)
R
mTH-Cre-AAV+ AAV-Ef1a-DIO-hM3Dq-mcherry
LC
S
Male
mCherry/TH/DAPI
LC-Merge
mCherry
TH
DAPI
4V
LC
T
U
V
W
Vehicle+Vehicle(icv.)
CNO+Vehicle(icv.)
CNO+Prazosin(icv.)
Vehicle+Prazosin(icv.)
Vehicle+Vehicle(VLPO)
CNO+Vehicle(VLPO)
CNO+Prazosin(VLPO)
Vehicle+Prazosin(VLPO)
X
Female
mCherry/TH/DAPI
LC-Merge
TH
mCherry
DAPI
4V
LC
Y
Z
Vehicle+Vehicle(VLPO)
CNO+Vehicle(VLPO)
CNO+Prazosin(VLPO)
Vehicle+Prazosin(VLPO)

Figure 6. ICV injection or intra-VLPO microinjection of α1-R antagonist reverses the pro-recovery effect of optogenetic or chemogenetic of activation LCNE neurons

(A) A schematic of intracerebroventricular injection of different noradrenergic receptor agonists and antagonists.

(B) A representative photomicrograph showing the tracks of cannulas implanted into the lateral ventricle.

(C-H) Results showed the effects of intracerebroventricular injection of different doses of phenylephrine, prazosin, clonidine, yohimbine, isoprenaline, and propranolol on the recovery time of midazolam.

(I) Results showed the effects of intracerebroventricular injection of phenylephrine (20mg/mL) and different doses of propranolol on the recovery time of midazolam.

(J) Protocol for photostimulation of LCNE neurons and intracerebroventricular injection or intra-VLPO microinjection of α1-R antagonist.

(K, L) Schematic of the brief process of optogenetic activation and the representative photomicrograph showing microinjection and optical fiber locations of the co-expression of hChR2 and TH in the LC.

(M, O) A representative photomicrograph showing the tracks of cannulas implanted into the lateral ventricle and bilateral VLPO.

(N, P) Results showed the effects of photostimulation of LCNE neurons and intracerebroventricular injection or intra-VLPO microinjection of prazosin on the recovery time of midazolam.

(Q) Protocol for chemogenetic activation of LCNE neurons and intracerebroventricular

injection or intra-VLPO microinjection of an α1-R antagonist.

(R, S) Schematic of the location of virus injection and the representative photomicrograph showing the co-expression of hM3Dq and TH in the LC of male mice.

(T, V) A representative photomicrograph showing the tracks of cannulas implanted into the lateral ventricle and bilateral VLPO in the male mice.

(U, W) Results showed the effects of chemogenetic activation of LCNE neurons and intracerebroventricular injection or intra-VLPO microinjection of prazosin on the recovery time of midazolam in male mice.

(X, Y) A representative photomicrograph showing the co-expression of hM3Dq and TH in the LC and the tracks of cannulas implanted into the bilateral VLPO in the female mice.

(Z) Results showed the effects of chemogenetic activation of LCNE neurons and intra-VLPO microinjection of prazosin on the recovery time of midazolam in female mice.

icv: intracerebroventricular; PS: photostimulation; *$p<0.05$; **$p<0.01$; ***$p<0.001$

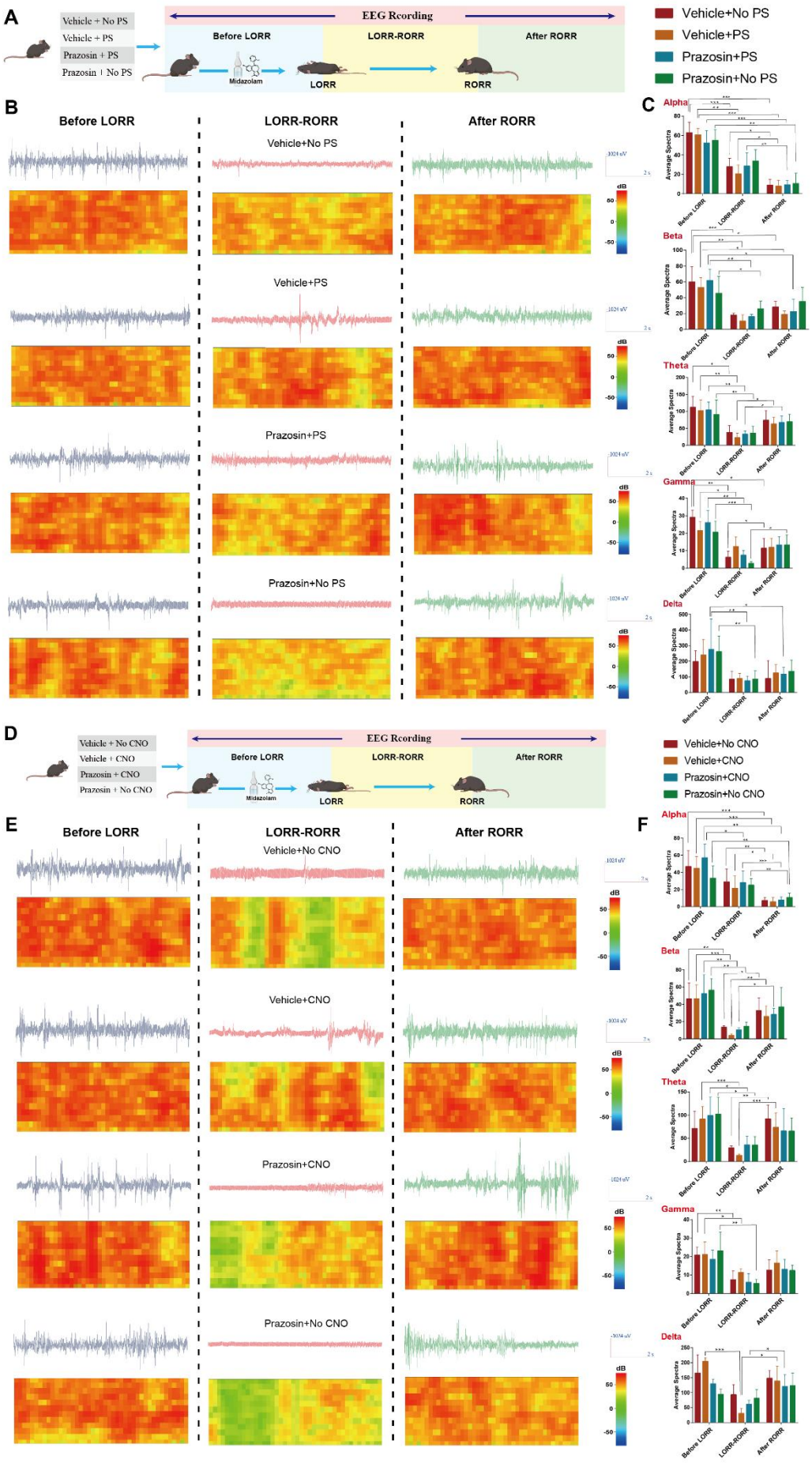
A
Vehicle + No PS
Vehicle + PS
Prazosin + PS
Prazosin + No PS
EEG Rcording
Before LORR
LORR-RORR
After RORR
Midazolam
LORR
RORR
Vehicle+No PS
Vehicle+PS
Prazosin+PS
Prazosin+No PS
B
Before LORR
LORR-RORR
After RORR
Vehicle+No PS
Vehicle+PS
Prazosin+PS
Prazosin+No PS
dB
C
Alpha
Beta
Theta
Gamma
Delta
Average Spectra
Before LORR
LORR-RORR
After RORR
D
Vehicle + No CNO
Vehicle + CNO
Prazosin + CNO
Prazosin + No CNO
EEG Rcording
Before LORR
LORR-RORR
After RORR
Midazolam
LORR
RORR
Vehicle+No CNO
Vehicle+CNO
Prazosin+CNO
Prazosin+No CNO
E
Before LORR
LORR-RORR
After RORR
Vehicle+No CNO
Vehicle+CNO
Prazosin+CNO
Prazosin+No CNO
dB
F
Alpha
Beta
Theta
Gamma
Delta
Average Spectra
Before LORR
LORR-RORR
After RORR

Figure 7. Effect of ICV injection of α1-R antagonist and activation of LCNE neurons on EEG activity

(A, D) Schematic diagram of EEG recording method.

(B) EEG and spectrum of mice in vehicle+no PS, vehicle+PS, Prazosin+no PS, and Prazosin+PS at the Before LORR, LORR-RORR, and After RORR stages.

(C) Alpha, Beta, Theta, Gamma, and Delta wave proportion of EEG in four groups of mice in different stages.

(E) EEG and spectrum of mice in vehicle+no CNO, vehicle+ CNO, Prazosin+no CNO, and Prazosin+ CNO at the Before LORR, LORR-RORR, and After RORR stages.

(F) Alpha, Beta, Theta, Gamma, and Delta wave proportion of EEG in four groups of mice in different stages.

PS: photostimulation; *$p<0.05$; **$p<0.01$; ***$p<0.001$

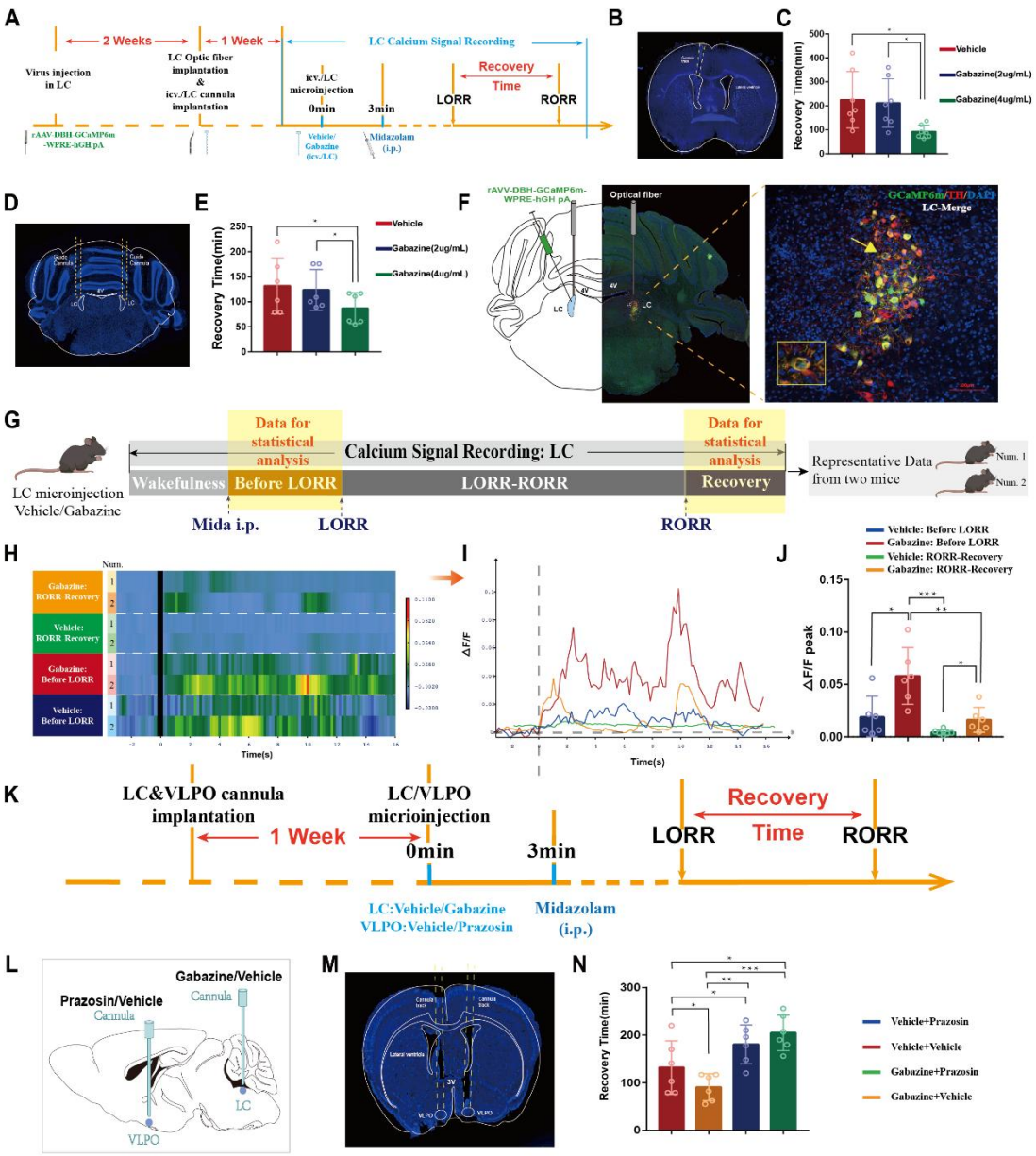

Figure 8. GABAA-R is an important mechanical binding site for midazolam in the LC

(A) Protocol for the fiber optic recording of calcium signals in the LC after intracerebroventricular injection or intra-LC microinjection of different doses of gabazine.

(B, D) A representative photomicrograph showing the tracks of cannulas implanted into the lateral ventricle and the bilateral LC.

(C, E) Results showed the effects of ICV injection or intra-LC microinjection of different doses of gabazine on the recovery time of midazolam.

(F) A representative photomicrograph showing the microinjection and optical fiber locations and the co-expression of GCaMP6s and TH in the LC.

(G) Schematic diagram of the method of recording the calcium signal at the LC, and sources of statistical data.

(H) A heatmap of calcium signaling changes in bilateral LCNE neurons induced by midazolam with or without intracerebroventricular injection of gabazine. (vehicle group: n=2; gabazine group: n=2; Calcium signaling data from two representative mice per group. Calcium signaling information of each mouse in the stage Before RORR and R-Recovery were selected for presentation and further statistical analysis.)

(I) A statistical diagram of calcium signaling changes in bilateral LC with or without intracerebroventricular injection of gabazine.

(J) The peak ΔF/F in the Before RORR and RORR-Recovery stages with or without intracerebroventricular injection of gabazine.

(K) Propofol for intra-LC microinjection of GABAA-R antagonist and intra-VLPO microinjection of α1-R antagonist.

(L) A schematic of the position of cannula implantation.

(M) A representative photomicrograph showing the tracks of cannulas implanted into the bilateral VLPO.

(N) Results showed the effects of intra-LC injection of gabazine and intra-VLPO injection of prazosin on the recovery time of midazolam.

icv: intracerebroventricular; *$p<0.05$; **$p<0.01$; ***$p<0.001$

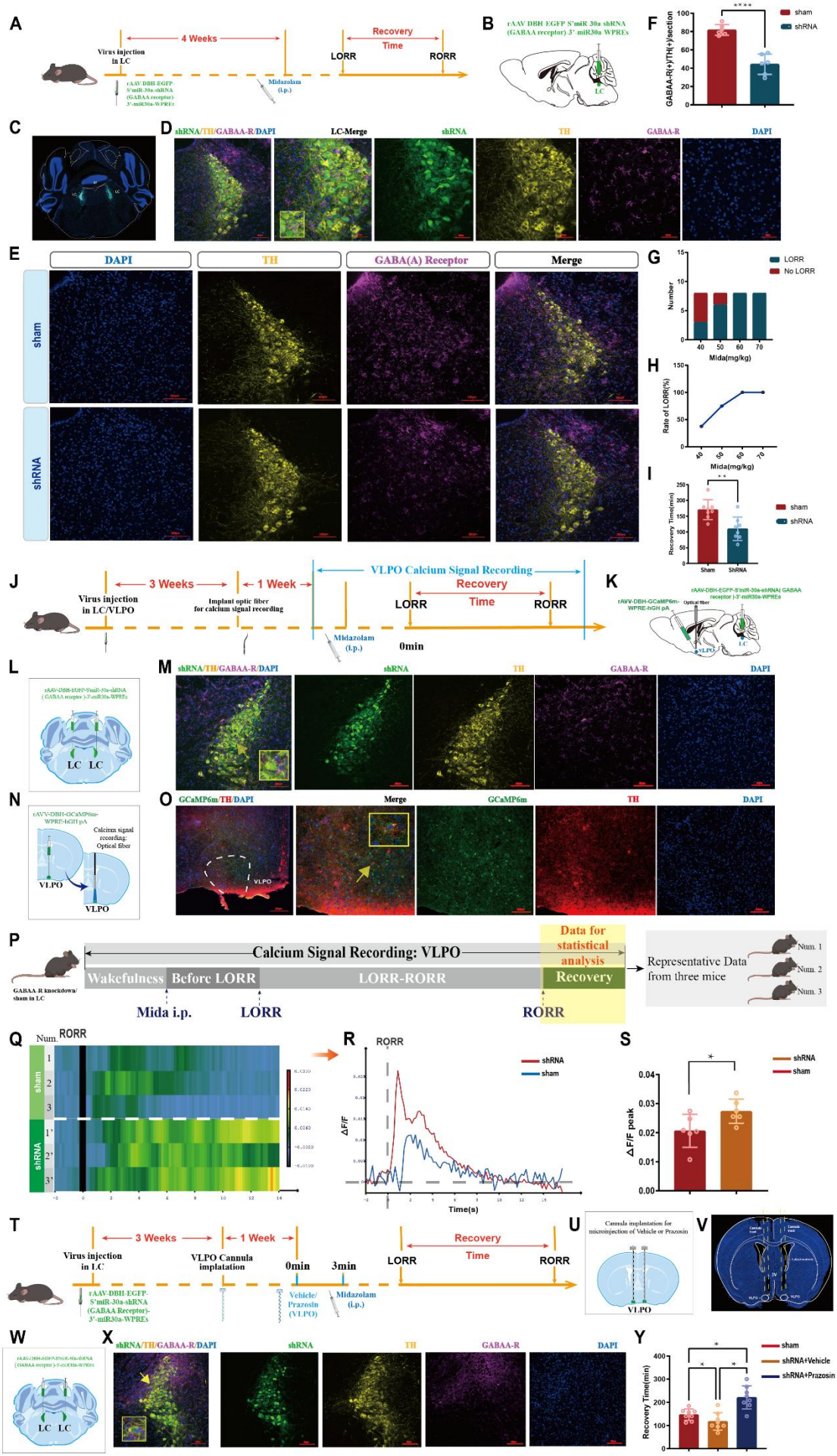
A
4 Weeks
Virus injection in LC
Recovery Time
LORR
RORR
Midazolam (i.p.)
B
rAAV DBH EGFP S'miR 30a shRNA (GABAA receptor) 3' miR30a WPREs
LC
F
GABAA-R(+)/TH(+)/section
sham
shRNA
C
D
shRNA/TH/GABAA-R/DAPI
LC-Merge
shRNA
TH
GABAA-R
DAPI
E
DAPI
TH
GABA(A) Receptor
Merge
sham
shRNA
G
LORR
No LORR
Number
Mida(mg/kg)
H
Rate of LORR(%)
Mida(mg/kg)
I
Recovery Time(min)
Sham
ShRNA
J
3 Weeks
1 Week
VLPO Calcium Signal Recording
Virus injection in LC/VLPO
Implant optic fiber for calcium signal recording
Recovery Time
LORR
RORR
Midazolam (i.p.)
0min
K
rAAV-DBH-GCaMP6m-WPRE-hGH pA
rAAV-DBH-EGFP-S'miR-30a-shRNA(GABAA receptor)-3'-miR30a-WPREs
Optical fiber
VLPO
LC
L
rAAV-DBH-EGFP-S'miR-30a-shRNA (GABAA receptor)-3'-miR30a-WPREs
LC LC
M
shRNA/TH/GABAA-R/DAPI
shRNA
TH
GABAA-R
DAPI
N
rAAV-DBH-GCaMP6m-WPRE-hGH pA
Calcium signal recording: Optical fiber
VLPO
VLPO
O
GCaMP6m/TH/DAPI
Merge
GCaMP6m
TH
DAPI
VLPO
P
Calcium Signal Recording: VLPO
Data for statistical analysis
Wakefulness
Before LORR
LORR-RORR
Recovery
GABAA R knockdown/ sham in LC
Mida i.p.
LORR
RORR
Representative Data from three mice
Num. 1
Num. 2
Num. 3
Q
Num.
RORR
sham
shRNA
R
RORR
shRNA
sham
ΔF/F
Time(s)
S
shRNA
sham
ΔF/F peak
T
3 Weeks
1 Week
Virus injection in LC
VLPO Cannula implatation
0min
3min
Recovery Time
LORR
RORR
rAAV-DBH-EGFP-S'miR-30a-shRNA (GABAA Receptor)-3'-miR30a-WPREs
Vehicle/ Prazosin (VLPO)
Midazolam (i.p.)
U
Cannula implantation for microinjection of Vehicle or Prazosin
VLPO
V
W
rAAV-DBH-EGFP-S'miR-30a-shRNA (GABAA receptor)-3'-miR30a-WPREs
LC LC
X
shRNA/TH/GABAA-R/DAPI
shRNA
TH
GABAA-R
DAPI
Y
sham
shRNA+Vehicle
shRNA+Prazosin
Recovery Time(min)

Figure 9. GABA-ergic and NE-ergic systems interact with each other, co-regulate the recovery from midazolam

(A) Protocol for exploring the influence of knocking down the GABAA-R on the recovery time from midazolam.

(B-C) Schematic diagram and the representative photomicrograph showing the position of virus injection.

(D) A representative photomicrograph showing the co-expression of shRNA， TH， and GABAA-R in the LC.

(E) Representative photomicrograph of the difference of GABAA-R expression in the LC after shRNA-mediated knockdown.

(F) The quantification of GABAA-R (+)/TH (+) cells in the LC between the shRNA group and the sham group.

(G) Number of LORR and no LORR induced by different doses of midazolam in GABAA-R knockdown mice.

(H) Rate of LORR (%) in GABAA-R knockdown mice at different doses of midazolam.

(I) The statistical bar shows shRNA-mediated GABAA-R knockdown effect on the recovery time from midazolam.

(J-K) Protocol for exploring the calcium signals changes in the VLPO after knocking down the GABAA-R.

(L-M, N-O) Schematic diagram and the representative photomicrograph showing the position of virus injection and the co-expression of shRNA， TH， and GABAA-R in the LC.

(N-O) Schematic diagram of the brief process of calcium signal recording and the

representative photomicrograph showing the co-expression of GCaP6m and TH in the VLPO.

(P) Schematic diagram of the method of recording the calcium signal at the VLPO, and sources of statistical data.

(Q-R) Heatmap and statistical diagram of calcium signaling changes in bilateral VLPO at the after RORR stage with or without knocking down GABAA-R on LCNE neurons. (Showing changes in calcium signaling during the RORR and the Recovery period; shRNA group, n=3; sham group, n=3)

(S) The peak ΔF/F in the VLPO with or without knocking down GABAA-R on LCNE neurons.

(T) Protocol for exploring the effect of blocking α1-R in the VLPO and knocking down the GABAA-R in the LC on the recovery time from midazolam.

(U-V) Schematic diagram and the representative photomicrograph showing the positions of cannula implantation.

(W-X) Schematic diagram and the representative photomicrograph showing the position of virus injection and the co-expression of shRNA， TH， and GABAA-R in the LC.

(Y) Results showed recovery time between sham, shRNA + Vehicle, and shRNA + Prazosin.

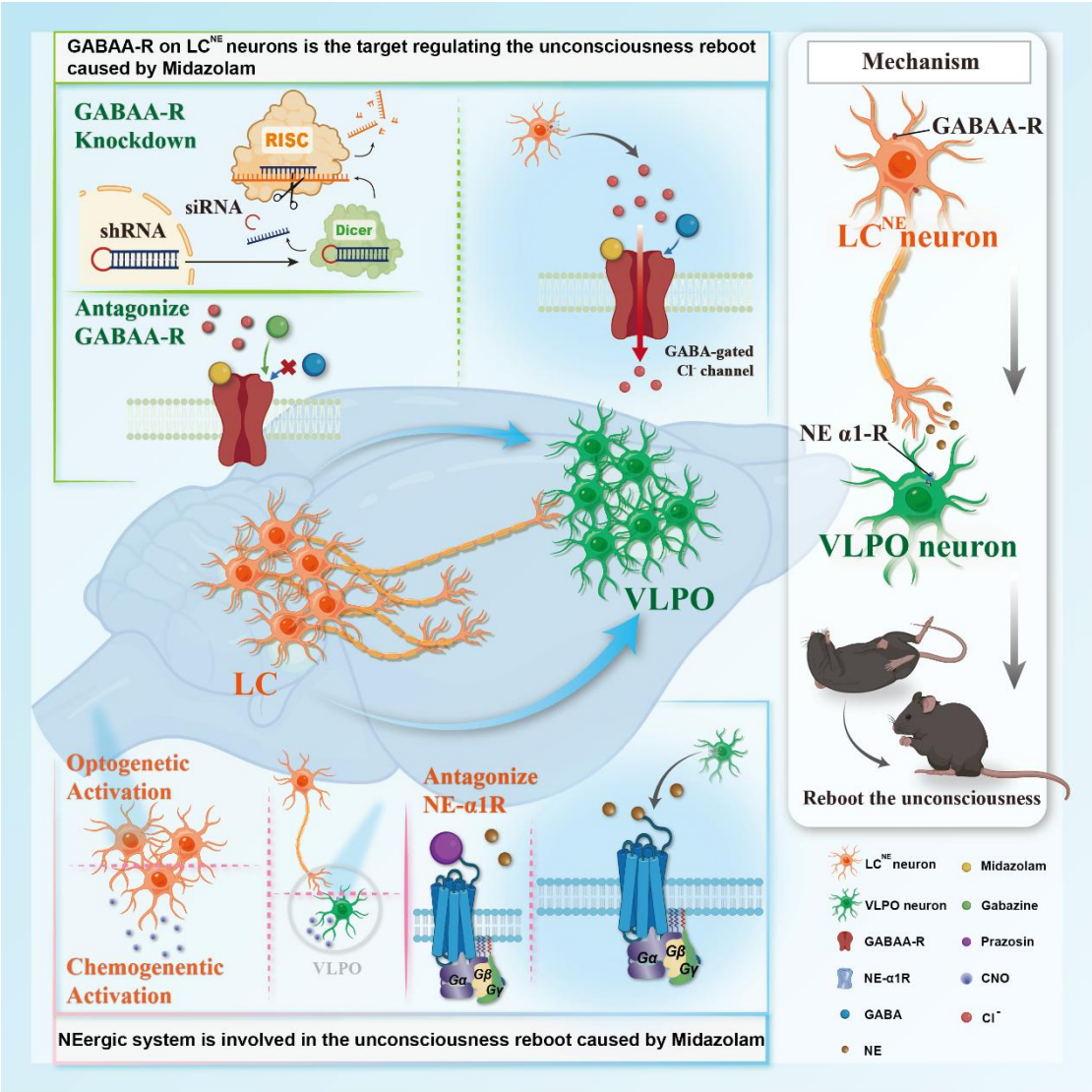

Summary

By using pharmacology, optogenetics, chemogenetics, fiber photometry, and gene knockdown, we revealed the role of locus coeruleus (LC)-ventrolateral preoptic nucleus (VLPO) noradrenergic neural circuit in regulating midazolam-induced altered consciousness. This effect was mediated by α1 adrenergic receptors. Moreover, gamma-aminobutyric acid receptor type A (GABAA-R) is a mechanistically important binding site in the LC for midazolam.